Quantum Fluctuations in Optical Systems

P.L. Knight
Optics Section, Blackett Laboratory, Imperial College,
London SW7 2BZ, England

March 4, 1996

Contents

1 Introduction **2**

2 Quantum Interference and the Construction of Nonclassical States **3**

2.1 Nonclassical Light, Quadratures and Phase–Sensitive Observables 3
2.2 Phase–Space and Quasi–Probabilities 13
2.3 Quantum Noise as a Stochastic Process 15
2.4 Marginal distributions and reconstruction of Wigner functions . . 18
2.5 Joint Measurements of p, q in Phase Space 20
2.6 Phase–Space Sampling Entropies 27
2.7 Mutual Information and Entropic Uncertainty 28
2.8 Building Nonclassical States by Quantum Interference 30

3 Dissipation Versus Coherent Evolution: Decoherence **36**

4 Unravelling the Master Equation **37**

5 Quantum Jumps **43**

5.1 Intrinsic or Extrinsic Jumps 43
5.2 Observation of Quantum Jumps 44

6 Quantum State Diffusion **51**

7 Comparison of Ensemble Averaged Results **60**

8 Entanglement in Quantum Optics **63**

8.1 Entanglement 63
8.2 The Schmidt Decomposition 65
8.3 Two-mode Squeezed State 69
8.4 Entangled Fields and Atoms 72
8.5 Jaynes-Cummings Model 74
8.6 Perspective on Schmidt Decomposition 78
8.7 Conditional measurements and entangled photon pairs 79

9 Conclusions **81**

1 Introduction

In these lectures, I was asked by the organizers of the School to provide the introductory material needed to describe quantum fluctuations and noise in optical fields and then to describe current work on non–classical radiation. I start by describing the basic machinery of field quantization as simply as I can, and review the nature of field modes and their fluctuations. A common theme which runs through these lectures is the use of phase–space in quantum optics to characterize quantum fluctuations. I show how nonclassical fields can be described in particular by the Wigner quasiprobability, and discuss the problem of how nonclassical light fields can be studied in phase–space. I then turn to the problem of how to construct nonclassical states by quantum interference. In practice, we never consider totally isolated quantum systems: they are always embedded in a dissipative environment, and this is the next topic I discuss, followed by a treatment of the time–evolution of the individual quantum systems within an ensemble. The master equation describing an ensemble of systems interacting with an open environment is "unravelled" into individual quantum trajectories which, depending on the manner in which the information is gathered about their evolution, either localize stochastically or exhibit quantum jumps. Finally I discuss the problem of *entanglement* of interacting subsystems (such as two field modes, or a field and an atom) in quantum optics.

It is quite difficult to provide a truly convincing definition of nonclassical states of light. In a real sense, *all* states of light contain some feature which is demonstrably quantum–mechanical in origin which derives from discreteness of the energy quanta which make up the field. But in practice, these non–classical features are hard to measure [1]. Many fields can be modelled reasonably accurately as *classical* fluctuating objects and their measurable properties are influenced hardly at all by their underlying quantum nature. Coherent and thermal fields are examples whose quantum characteristics are, for most practical purposes, invisible. Nevertheless, these fields *are* inherently quantum mechanical and their underlying quantum properties are recoverable at least in principle, through careful scrutiny of their statistics (for example using a micromaser). However, there *are* classes of light field states which are generally agreed to be wholly nonclassical: their *gross* properties (for example the photon number or field quadrature variances) are *below* that of a perfectly-coherent field. These sub-Poissonian and squeezed states have been a central theme in quantum optics in the past two decades, [1]. In these lectures we will demonstrate how nonclassical field states may be constructed by superposing component states in phase-space [2]. We will then describe how these nonclassical states are peculiarly sensitive to dissipation when the coupling of the field modes to their larger environment [3] is taken into account. Well before the field energy is significantly dissipated, the coherences responsible for the nonclassical behaviour will decay, at a "decoherence rate" [4] determined by the square of the separation of the constituent components of the nonclassical superpositions in phase-space.

The traditional view of decoherence deals with the ensemble: but in quantum optics it is quite feasible to examine the behaviour of *individual* members of the ensemble. For example we may examine the state of a single trapped laser cooled ion, or of a field mode in a high–Q cavity. We address these questions using newly-developed ideas of "quantum trajectories" (see e.g. [5]). In doing so, we show how the dissipative environment "deconstructs" the field into its appropriate constituent parts. Finally we examine the problem of entanglement of interacting subsystems in quantum optics, and show how this modifies the quantum dynamics and especially the fluctuations of individual subsystems.

2 Quantum Interference and the Construction of Nonclassical States

2.1 Nonclassical Light, Quadratures and Phase–Sensitive Observables

We commence our discussion by examining how a single light field mode of frequency ω is quantized in a box of volume V. This is described by the field operator [6]

$$\hat{E} = (\frac{2\omega^2}{\epsilon_0 V})^{\frac{1}{2}}\, \hat{q}\, \sin kz \tag{1}$$

where ϵ_0 the permittivity of free space and $k = \omega/c$ the wavevector; $\hat{q}$ is an Hermitian operator having the dimension of a length. This can be expressed in terms of annihilation ($\hat{a}$) and creation operators ($\hat{a}^\dagger$) as

$$\hat{E} = \sqrt{2}\mathcal{E}_0\, \sin kz\, \{\hat{a}\, \mathrm{e}^{-i\omega t} + \hat{a}^\dagger\, \mathrm{e}^{i\omega t}\} \tag{2}$$

where

$$\hat{a} = (2\hbar\omega)^{-\frac{1}{2}}(\omega\hat{q} + i\hat{p}), \qquad [\hat{a}, \hat{a}^\dagger] = 1 \tag{3}$$

where $\hat{p}$ is a conjugate field variable to $\hat{q}$. The quantity

$$\mathcal{E}_0 = (\frac{\hbar\omega}{2\epsilon_0 V})^{\frac{1}{2}}$$

is the "electric field per photon" and describes the quantum unit of electric field strength. As an example of the magnitude of this electric field per photon, let us consider visible radiation in a $10^{-2}cm$ cavity, where we find $\mathcal{E}_0 = 0.6Vcm^{-1}$ which corresponds to an effective intensity of $(1/2)mWcm^{-2}$. Even if all sources of radiation are turned off, each mode posesses a minimum field, randomly fluctuating with a zero mean, and an rms value of $\mathcal{E}_0$. The number states of the field $|n\rangle$ may be described by the number of excitations n which govern the energy of the n-quantum state $E_n = (n + \frac{1}{2})\hbar\omega$ [7].

A phase insensitive detector (a photomultiplier or photodiode) gives us information about the mean intensity $\langle I\rangle = \langle E^{(-)}E^{(+)}$ where $E^{(-)}\rangle$ contains (apart from a mode normalization factor) the field annihilation operator, and about the intensity fluctuations $\Delta I = [\langle I^2\rangle - \langle I\rangle^2]^{\frac{1}{2}}$. These can be translated into equivalent quantities for the mean photon number $\langle n\rangle$ and its standard deviation Δn. A perfectly coherent light field has Poissonian statistics [7] with number probabilities $p(n)$

$$p(n) = \frac{\langle n\rangle^n}{n!}\exp(-\langle n\rangle) \tag{4}$$

so that $\langle n^2\rangle - \langle n\rangle^2 = \langle n\rangle$ as expected (this is sometimes called the "particle" term in Einstein's counting formula). A thermal (chaotic) field has the probability distribution given by the Bose–Einstein form

$$p(n) = \frac{\langle n\rangle^n}{(1+\langle n\rangle)^{n+1}} \tag{5}$$

so that $\langle n^2\rangle - \langle n\rangle^2 = \langle n\rangle^2 + \langle n\rangle$; the additional term represents the photon bunching of thermal light. Much work has been done on photon counting, from the early photon bunching experiments of Hanbury, Brown and Twiss (see eq.[8]) to the realization of non–classical *antibunched* and sub–Poissonian light sources [7], in which $\Delta n < \langle n\rangle^{\frac{1}{2}}$. These are discussed elsewhere in these proceedings by Davidovich.

A striking example of antibunching is given by the experiment by Grangier, Roger and Aspect [9] in which an atomic source of single photons is used to demonstrate that photons cannot be split by a beam splitter. In this experiment, single photons are incident on a beam splitter as shown in Fig. 1.

The input to the beam splitter is a single photon (and a vacuum state of the other input port). The output in the two mode is the *entangled* state

$$|out\rangle = \frac{1}{\sqrt{2}}(|0\rangle_r|1\rangle_t + |1\rangle_r|0\rangle_t) \tag{6}$$

where r, t stand for reflected and transmitted modes. The normalized coincidence rate is governed by the second order coherence function:

$$g_{rt} = \langle a_r^\dagger a_t^\dagger a_r a_t\rangle. \tag{7}$$

For the single photon input, of course, $g_{rt} = 0$: we either see a reflected *or* a transmitted mode excitation. Single photons cannot be split. The experiments of Grangier et al ([9]) see just this indivisibility of photons. When this is translated into intensities, we see this implies that the mean square intensity is less than the square of the mean, something impossible for a fluctuating optical field described by a classical stochastic process. When the beam–splitter–counter geometry is replaced by a Mach–Zehnder interferometer geometry, Grangier et al

Figure 1: Schematic outline of Grangier et al experiment to beam–split a single photon: an atomic source S emits *pairs* of photons of frequency ν_1 and ν_2. The ν_1 photon is used as a gate of duration Δt for the coincidence counters of the ν_2 photon. Detector D_r counts reflected photons (with number N_r), detector D_t counts transmitted photons (with number N_r); the coincidence counts are denoted N_c.

Figure 2: Homodyne mixing of a system field of interest E_s with a local field of amplitude E_l and adjustable phase χ by a beam splitter of transmissivity t and reflectivity r.

see then the fringe pattern built up one photon at a time ([10]). The interference pattern is built up from one photon events; even though there was never more than one photon at a time in the apparatus, the fringe structure remains undiminished.

Instead of direct, phase–independent detection of intensities or of photon numbers, one can interfere the light field of interest with a reference beam from a well–stabilized local oscillator. This is the basis for homodyne (if fields have the same frequency), or heterodyne (if fields have different frequencies) phase–sensitive detection. Consider the scheme shown in Fig. 2.

The field $(tE_s + rE_l)$ shown in Fig. 2 is detected by a square law device responding to the intensity. The detected signal thus contains a beat note, or interference term

$$I_i \sim \langle E_s E_l^* e^{i\chi} + c.c. \rangle. \tag{8}$$

If the local oscillator is prepared in a coherent state with a large amplitude, we can with confidence regard the local oscillator field as a classical field, so that

this can be factored out of the expectation value as

$$I_i \sim E_l(\langle E^{(-)}\rangle e^{-i\chi} + \langle E^{(+)}\rangle e^{+i\chi}) \quad (9)$$

$$= E_l\langle E(\chi)\rangle \quad (10)$$

so that the phase–dependence of the system–field can be mapped out by varying the local oscillator phase χ. We can investigate its variance by studying the intensity fluctuations (or their noise spectrum). Normally $rE_l \gg t\langle E\rangle$ so that the detected intensity $\langle I_d\rangle$ (or detected photon number $\langle n_{det}\rangle$) is given by [8]

$$\langle I_d\rangle \cong |r|^2|E_l|^2 + |t||r||E_l|\langle E(\chi)\rangle. \quad (11)$$

A suitable choice of phase angle χ allows us to read off the value of the system quadrature X and Y directly. The photon number fluctuations are given by

$$\langle \Delta n\rangle_{det} \sim |r|^2|E_l|^2\{|r|^2 + 4|t|^2\langle(\Delta E(\chi))^2\rangle\}. \quad (12)$$

If the quantum noise on the system–field is phase dependent (as it is for squeezed light), then as χ is varied, the number fluctuations also vary and for some phase angles these are reduced below that of the normal coherent state "shot noise" result. We will return to the problem of phase sensitive field detection in section 2.5.

The time-dependence $\exp(\pm i\omega t)$ in eq. (2) may be regarded as a *phase* dependence: we can write $\omega t = \chi$, and imagine χ to describe the general phase-dependence of the electric field through the generalization of eq. (2) [8],

$$\hat{E}(\chi) = \sqrt{2}\mathcal{E}_0 \sin kz\,(\hat{a}\,e^{-i\chi} + \hat{a}^\dagger\,e^{i\chi}) \quad (13)$$

where the phase χ may be that due to temporal evolution or due to the insertion of optical elements, such as a glass wedge or other device, in an experimental situation to retard the field. Because the field annihilation and creation operators do not commute, we see that the total electric field operators evaluated at different phase-angles also do not commute:

$$[\hat{E}(0), \hat{E}(\chi)] = i\,4\mathcal{E}_0^2 \sin\chi \quad (14)$$

so that the associated field uncertainties $\Delta E(0)$ and $\Delta E(\chi)$ must satisfy the uncertainty relation

$$\Delta E(0)\,\Delta E(\chi) \geq 2\mathcal{E}_0^2\,|\sin\chi|\,. \quad (15)$$

For most electromagnetic field states, such as coherent states or number states, the field uncertainty is *independent* of the field phase χ : the quantum noise is phase-independent. But if the field uncertainty at one choice of phase (say $\chi = 0$) is manipulated to be small (compared with $\mathcal{E}_0$), then at a later field phase angle the uncertainty is correspondingly increased (Fig. 3): this is the basis of *squeezed light* [8]. Note that those phase angles where the quantum

Figure 3: Phase-dependent quantum noise of squeezed light

noise is reduced below $\mathcal{E}_0$ occur periodically to satisfy the sinusoid of eq. (15).

It is convenient to parametrize the field in terms of the Hermitian *quadrature* operators $\hat{X}, \hat{Y}$ instead of the non-Hermitian annihilation and creation operators $\hat{a}, \hat{a}^\dagger$ so that

$$\hat{E} = 2^{\frac{3}{2}} \mathcal{E}_0 \, \sin kz \, (\hat{X} \cos \omega t + \hat{Y} \sin \omega t) \tag{16}$$

where

$$\hat{X} = \frac{1}{2} \, (\hat{a} + \hat{a}^\dagger) \, , \qquad \hat{Y} = \frac{1}{2i} \, (\hat{a} - \hat{a}^\dagger) \tag{17}$$

$$[\hat{X}, \hat{Y}] = \frac{i}{2} \tag{18}$$

and

$$\Delta X \, \Delta Y \geq \frac{1}{4} \, . \tag{19}$$

For the vacuum state, or any coherent state $|\alpha\rangle$ formed by a displacement of the vacuum by an amplitude α from the origin in *phase-space*, $\Delta X = \Delta Y = \frac{1}{2}$. The c-number variables X, Y characterize the phase-space of the field mode. The coherent state $|\alpha\rangle$ has mean quadratures X_0, Y_0 and uncertainties $\Delta X = \frac{1}{2} = \Delta Y$ and is portrayed in phase-space in Fig. 4. In what follows, we will relate the shaded "error contour" in Fig. 4 to the Wigner function phase-space quasiprobability $W_\Psi(q,p)$, where

$$\hat{X} \;\; = \;\; (\frac{\omega}{2\hbar})^{\frac{1}{2}} \, \hat{q} \tag{20}$$

$$\hat{Y} \;\; = \;\; (2\hbar\omega)^{-\frac{1}{2}} \, \hat{p} \, . \tag{21}$$

The phase-space description of an oscillator such as the field mode implies a joint probability distribution for the measurement of the canonical coordinates q and p. At this point, we need to deal with the lack of commutativity of position and momentum in quantum mechanics and the concomitant non-existence of a positive joint probability distribution. The Wigner function, $W_\Psi(q,p)$, introduced in 1932, is defined for a pure state as [11]

$$W_\Psi(q,p) = \int \frac{dq'}{2\pi\hbar} \, \Psi^*(q + q'/2) \, \Psi(q - q'/2) \, \mathrm{e}^{ipq'/\hbar} \, . \tag{22}$$

Although this can only be regarded at best as a quasiprobability (it may be negative in some areas of phase-space), it does generate the measurable marginal distributions $|\Psi(q)|^2$ and $|\Psi(p)|^2$ on integration over p and over q respectively. Indeed, the negativity of the Wigner functions for some states can be regarded as a signature of their non-classicality. However, the only pure state Wigner functions which are positive everywhere are Gaussian [12]: i.e. restricted to coherent states and the squeezed states (generated by the quadratic squeeze operator which preserves the minimum uncertainty product $\Delta X \Delta Y = 1/2$). In Fig. 5, we show the Wigner function for the nine-photon Fock state: this is a

Figure 4: Phase-space portrait of a coherent state of amplitude (X_0, Y_0) and fluctuations $\Delta X, \Delta Y$

Figure 5: Wigner function for the nine-photon Fock state.

rotationally-symmetric Laguerre polynomial, with a large outer "rim" situated at a radius $\sqrt{n} = 3$ and a sequence of fringes including substantial negative regions.

It is not really necessary to describe the details of how squeezing is realized in practice: this was reviewed in great detail by Kimble at the previous Les Houches Summer School devoted to quantum optics, [13]. Nevertheless, it may be useful to present a brief reminder of the essentials. To reduce the quantum noise of an optical field requires some kind of nonlinearity (linear absorption reduces the intensity and in general increases the noise). The optimum seems to be processes which create or destroy photons in pairs. Canonical squeezing (*i.e.* squeezing which preserves commutators and maintains minimum uncertainty characteristics) should be of the form

$$X \longrightarrow X' = Xe^{-s} \tag{23}$$

$$Y \longrightarrow Y' = Ye^{+s} \tag{24}$$

so that the basic commutation relation is preserved, whilst

$$\langle (\Delta X)^2 \rangle = \frac{1}{4} e^{-2s} \tag{25}$$

$$\langle (\Delta Y)^2 \rangle = \frac{1}{4} e^{+2s} \tag{26}$$

which preserves the minimum uncertainty. Noise compression of this kind can be generated by the squeezing operator

$$\hat{S}(\xi) = \exp(\frac{1}{2}\xi \hat{a}^2 - \frac{1}{2}\xi (\hat{a}^\dagger)^2) \tag{27}$$

where in general the squeeze parameter $\xi = s\exp(i\theta)$. The squeezed vacuum $|\xi\rangle$ is generated from the conventional vacuum by

$$\hat{S}(\xi)|0\rangle = |s\rangle \tag{28}$$

Quadratic variances are changed by such a squeeze operator as [8]

$$\langle (\Delta X)^2 \rangle = \frac{1}{4}\{e^{-2s}\cos^2\frac{1}{2}\theta + e^{+2s}\sin^2\frac{1}{2}\theta\} \tag{29}$$

$$\langle (\Delta Y)^2 \rangle = \frac{1}{4}\{e^{-2s}\sin^2\frac{1}{2}\theta + e^{+2s}\cos^2\frac{1}{2}\theta\}. \tag{30}$$

For $\theta = 0$, we recover the result of eqs.(25) and (26). It is important to realize that in terms of the old (unsqueezed) variables, the squeezed vacuum contains photons:

$$\langle \xi | n | \xi \rangle = \langle a^\dagger a \rangle = \sinh^2 s. \tag{31}$$

The quadratic squeezing transformation of course generates photons in pairs, so that the squeezed vacuum contains only even photon numbers. Nonlinear optical interactions which implement this type of minimum uncertainty

state squeezing [1] include four–wave mixing, second harmonic generation and degenerate parametric amplification. For parametric amplification, the vacuum state evolves as $\exp(\frac{-i\mathcal{H}t}{\hbar})|0\rangle$ where $\mathcal{H}$ is the parametric Hamiltonian $\mathcal{H} = \chi^{(2)}\mathcal{E}\hat{a}^2 + h.c.$, where $\chi^{(2)}$ is the second order susceptibility for the parametric material (paramp for short) and $\mathcal{E}$ is the laser pump amplitude driving the paramp. The squeeze parameter ξ for this (oversimplified) model of parametric amplification is $\xi = 2i\chi^{(2)}\mathcal{E}t/\hbar$, and depends on the interaction time of the paramp process.

2.2 Phase–Space and Quasi–Probabilities

A classical stochastic model of fluctuating light fields centers on the joint probability density $P(q,p;t)$ for finding the field with quadratures X, Y or equivalently of "position" q and "momentum" p in phase space. This joint probability density is the true probability density: it is positive everywhere, is normalized, and can generate moments

$$\langle q^r p^s \rangle = \int_{-\infty}^{\infty} dq \int_{-\infty}^{\infty} dp\, q^r\, p^s\, P(q,p) \tag{32}$$

The situation in quantum physics is much more complicated as the canonical variables $\hat{q}$ and $\hat{p}$ do not commute and cannot be jointly specified to arbitrary accuracy. The Wigner function, which we introduced above, is essentially the simplest quantum analogue of the joint probability density $P(q,p;t)$. In particular, it generates the correct (absolute) marginal distributions for p and q. It is *not* however positive everywhere (except for the special case of a Gaussian) and cannot be regarded as a joint probability: it is, for this reason, regarded as a quasiprobability [3].

A classical joint probability $P(q,p;t) \equiv P(\alpha,\alpha^*;t)$ where α is some complex amplitude, can be related to a characteristic function $C(\beta,\beta^*;t)$ through the Fourier transform

$$C(\beta,\beta^*;t) = \int d^2\alpha\, \exp(\beta\alpha^* - \beta^*\alpha)\, P(\alpha,\alpha^*,t) \tag{33}$$

so that

$$C(\beta,\beta^*;t) = \langle \exp(\beta\alpha^* - \beta^*\alpha) \rangle \tag{34}$$

It would be tempting to generalize this for a quantum characteristic function

$$C(\beta,\beta^*;t) = Tr[\exp(\beta\hat{a}^\dagger - \beta^*\hat{a})\rho] \tag{35}$$

But $\hat{a}^\dagger$ and $\hat{a}$ do not commute, so there are a number of candidates: for example why not $Tr\{\exp(-\beta^*\hat{a})\exp(\beta\hat{a}^\dagger)\rho\}$? Different orderings generate different characteristic functions and different quasiprobabilities. Cahill and Glauber

[14] have shown how these can be grouped together by defining the "s–ordered" characteristic function $C(\beta, s)$ by

$$C(\beta, \beta^*; s) = Tr\{\exp(\beta\hat{a}^\dagger - \beta^*\hat{a})\rho\}\exp(-|\beta|^2\frac{s}{2}). \tag{36}$$

If $s = 0$ this generates the Wigner function W, whereas if $s = -1$ then we obtain the Glauber–Sudarshan diagonal P–function and if $s = +1$ then we obtain the Husimi, or Q–function.

For the Wigner function, the mean value of some observable $\hat{M}$ is given by

$$\langle M\rangle = Tr\{\hat{\rho}M\} = \frac{1}{\pi}\int d^2\beta W(\beta)M(\beta). \tag{37}$$

We note that the coherent states $|\alpha\rangle$ are generated by the Glauber displacement operator $\hat{D}(\alpha) = \exp(\alpha\hat{a}^\dagger - \alpha^*\hat{a})$ so that $|\alpha\rangle = \hat{D}(\alpha)|0\rangle$. The observable $\hat{M} = \hat{M}(\hat{q}, \hat{p})$ has as its phase–space counterpart $M(q, p) = M(\beta)$. The differential element $1/\pi(dRe\alpha)(dIm\alpha) = (1/2\pi\hbar)dqdp$. The Wigner function can be written as

$$W(\beta) = \frac{1}{\pi}\int C^W(\beta)\exp(\beta\eta^* - \beta^*\eta)\, d^2\eta \tag{38}$$

where $C^W(\beta)$ is the Weyl–ordered characteristic function

$$C^W(\eta) \equiv Tr[\hat{\rho}\hat{D}(\eta)] \tag{39}$$

so for example the Weyl–ordered product is the symmetric form [3]

$$\{\hat{a}^\dagger\hat{a}\}^W = \frac{1}{2}(\hat{a}^\dagger\hat{a} + \hat{a}\hat{a}^\dagger) \tag{40}$$

and

$$\langle\{\hat{a}^\dagger\hat{a}\}^W\rangle = \frac{1}{2}(\hat{a}^\dagger\hat{a} + \hat{a}\hat{a}^\dagger) = \frac{1}{\pi}\int d^2\beta\, W(\beta). \tag{41}$$

The marginals of the Wigner function for an oscillator with $\hat{a} = (2\hbar)^{-1/2}(\lambda\hat{q} + i\lambda^{-1}\hat{p}$ (where $\lambda = (m\omega)^{1/2}$ for a material oscillator of mass m) are

$$W(q) = \frac{1}{\lambda(2\pi\hbar)^{\frac{1}{2}}}\int dp\, W(q, p) = \frac{(2\pi\hbar)^{\frac{1}{2}}}{\lambda}\langle q|\hat{\rho}|q\rangle \tag{42}$$

and moments can be calculated from

$$\langle\hat{q}^n\rangle = \frac{\lambda}{(2\pi\hbar)^{\frac{1}{2}}}\int dq\, q^n\, W(q). \tag{43}$$

For coherent states,

$$\langle(\Delta q)^2\rangle = \langle\hat{q}^2\rangle - \langle\hat{q}\rangle^2 = \frac{\hbar}{2\lambda^2} = \hbar\sigma_q^2 \tag{44}$$

$$\langle(\Delta p)^2\rangle = \langle\hat{p}^2\rangle - \langle\hat{p}\rangle^2 = \frac{\hbar\lambda^2}{2} = \hbar\sigma_p^2 \tag{45}$$

so that $\langle(\Delta q)^2\rangle\langle(\Delta p)^2\rangle = \frac{\hbar^2}{4}$.

Consider two states $|\Psi\rangle$ and $|\Phi\rangle$ with Wigner functions $W_\Psi(\beta)$ and $W_\Phi(\beta)$. Then the overlaps can be written as

$$|\langle\Psi|\Phi\rangle|^2 = \left|\int dq\Psi^*(q)\Phi(q)\right|^2 = \frac{1}{(2\pi\hbar)}\int dqdpW_\Psi(q,p)W_\Phi(q,p). \tag{46}$$

We note that if $|\Psi\rangle$ and $|\Phi\rangle$ are orthogonal, so that $\langle\Psi|\Phi\rangle = 0$, then

$$\frac{1}{(2\pi\hbar)}\int dqdpW_\Psi(q,p)W_\Phi(q,p) = 0. \tag{47}$$

This tells us immediately that Wigner function in general cannot be positive everywhere. Indeed, the only Wigner function which is positive everywhere [12] is the Gaussian

$$W_\Psi(q,p) = \frac{1}{\sigma_q(\Psi)\sigma_p(\Psi)}\frac{1}{\sqrt{1-r^2}}\exp\{-\frac{1}{2(1-r^2)\hbar}[\frac{(p-\langle p\rangle)^2}{\sigma_p^2(\Psi)} \tag{48}$$

$$- 2r\frac{(p-\langle p\rangle)(q-\langle q\rangle)}{\sigma_q(\Psi)\sigma_p(\Psi)} - \frac{(q-\langle q\rangle)^2}{\sigma_q^2(\Psi)}]\} \tag{49}$$

for which $\sigma_p(\Psi), \sigma_q(\Psi)$ are related as

$$\sigma_q(\Psi)\sigma_p(\Psi) = \frac{1}{4(1-r^2)}, \tag{50}$$

i.e. the coherent states and the M.U.S. squeezed states.

The squeezing transformation $S(\xi)$ introduced earlier is a *canonical* transformation. The phase–space distributions are modified by such canonical transforms in an interesting way, which preserves areas in phase space. Examples of linear canonical transformations include rotations, translations *and* squeezes [15].

2.3 Quantum Noise as a Stochastic Process

We next consider the modification of a quantum-mechanical light field mode, described by an input field annihilation operator $\hat{a}_{\rm IN}$, by a (possibly nonlinear) system which we idealize as a "black box" as in Fig.6. Input-output theory must provide an algorithm for deriving all the statistical properties of the OUT fields from those of the IN fields. We write this as [16]

$$\hat{a}_\mu = f_\mu(\hat{a}_\nu)\,. \tag{51}$$

In a classical stochastic approach, a noisy input signal $\bar{\alpha}_\nu + \delta\alpha_\nu$ (where $\bar{\alpha}_\nu$ is the mean value and $\delta\alpha_\nu$ the "noise") leads to a modified output $\bar{\alpha}_\mu + \delta\alpha_\mu$

$$\alpha_\mu + \delta\alpha_\mu = f_\mu(\bar{\alpha}_\nu + \delta\alpha_\nu). \tag{52}$$

Figure 6: Input-output relation, where an input field $\hat{a}_{\rm IN}$ is transformed into an output field $\hat{a}_{\rm OUT}$ by a quantum black box.

If the input fluctuations are described by a probability distribution $P_{\rm IN}$, then for *classical* stochastic processes

$$P_{\rm OUT}(\alpha_\mu) = P_{\rm IN}(f_\mu^{-1}(\alpha_\nu)) \, . \tag{53}$$

A natural question to ask is whether such a transformation holds for quantum fluctuations [16]. In quantum physics, the input-output transformation should preserve the basic commutation relations: that is, it should be *canonical* :

$$[\hat{a}_i, \hat{a}_j^\dagger] = \delta_{ij} \, . \tag{54}$$

If we restrict ourselves to *linear* canonical transformations through the action of some function $\hat{f}$ so that

$$\hat{b}_i = f_i(\hat{a}_j, \hat{a}_k^\dagger) = u_{ij}\hat{a}_j + v_{ik}\hat{a}_k^\dagger + c_i \tag{55}$$

then the basic commutation relation is preserved provided

$$u_{nj}u_{mj}^* - v_{nj}v_{mj}^* = \delta_{nm} \, , \tag{56}$$

$$u_{nj}v_{mj} - v_{nj}u_{mj} = 0 \, . \tag{57}$$

A canonical transformation preserves volumes when acting in phase-space. We can represent this canonical transformation through the action of a unitary

transformation $\hat{U}$ (the Stone – von Neumann theorem)

$$\hat{b}_i = \hat{U}^\dagger \hat{a}_i \hat{U} \tag{58}$$

which can be written in terms of the generators $\hat{J}_k$ as

$$\hat{U} = \mathrm{e}^{-i\alpha_k \hat{J}_k} \, . \tag{59}$$

Then by expansion of eq. (59) in eq. (58), we find [16]

$$\hat{b}_i = \hat{U}^\dagger \hat{a}_i \hat{U} = \hat{a}_i - i\,\alpha_k\,[\hat{a}_i, \hat{J}_k] + \ldots \tag{60}$$

If we insist on a linear canonical transformation, we require

$$[\hat{a}_i, \hat{J}_k] \propto \hat{a}_i \, , \text{ or } \hat{a}_j^\dagger \text{ or } \hat{I} \, . \tag{61}$$

In other words, a linear canonical transformation $\hat{f}$ requires a generator $\hat{J}_k$ which is made up of the identity matrix $\hat{I}$, or a *linear* combination of $\hat{a}$ and $\hat{a}^\dagger$ (the displacement operators) or *bilinear* combinations of $\hat{a}$ and $\hat{a}^\dagger$ (the squeezing operators). The bilinear combinations are

$$J^{(a)} = -i\,(\hat{a}^2 - \hat{a}^{\dagger 2}) = \frac{i}{2}\,(q\frac{\partial}{\partial q} - p\frac{\partial}{\partial p}) \tag{62}$$

$$J^{(b)} = (\hat{a}^2 + \hat{a}^{\dagger 2}) = \frac{i}{2}\,(q\frac{\partial}{\partial q} + p\frac{\partial}{\partial p}) \tag{63}$$

and

$$J^{(c)} = \frac{1}{2}\,(\hat{a}^\dagger \hat{a} + \hat{a}\hat{a}^\dagger) \tag{64}$$

which generate the stretches and rotations shown in Fig. 7. At this point, we can address the question posed earlier: which phase-space quantum quasiprobability transforms like the classical version given by eq. (53)? Only the Wigner function has this transformation property [16]

$$W_{\mathrm{OUT}}(\alpha_\mu) = W_{\mathrm{IN}}(f_\mu^{-1}(\alpha_\nu)) \, . \tag{65}$$

Other quasiprobabilities used in quantum optics, such as the diagonal coherent-state Glauber-Sudarshan P distribution or the Husimi Q-function do not transform in this way [16], and this emphasises the special rôle the Wigner function plays in quantum mechanics. The Wigner function was constructed to have simple properties under Galilean transformations from the outset; we note here that this transformation property is retained in dissipative dynamics. Given a linear canonical transformation, quantum noise can be simulated as a complex random process. The procedure is simple: first change all operators $\hat{a}_\mu, \hat{a}_\nu^\dagger$ into complex random variables α_μ, α_ν^*, and secondly use the Wigner functions for a statistical description of the fluctuations. Whether such simulations are truly

Figure 7: Bilinear canonical transformations: stretches and rotations of patches in phase-space.

semiclassical [17] is to some extent a matter of taste. But this method is extremely powerful, and has been exploited in great detail by the Paris group who pioneered this approach in squeezing [17]. We should emphasise that this procedure only works for linear transformations, and that nonlinear effects strongly perturb the phase-space and render this simple transformation worthless.

2.4 Marginal distributions and reconstruction of Wigner functions

The measurable marginal distributions $|\Psi(q)|^2$ and $|\Psi(p)|^2$ are not sufficient, in general, to allow a full reconstruction of the Wigner function $W_\Psi(q,p)$. However, such a reconstruction *is* possible if the marginal distributions for the *rotated quadratures*

$$X_\theta = X\cos\theta + Y\sin\theta \tag{66}$$

$$Y_\theta = -X\sin\theta + Y\cos\theta \tag{67}$$

are measured, as shown in Fig. 8. The Wigner function can be written in terms of the quadratures X, Y as $W_\Psi(X,Y)$; or in rotated coordinates as $W_\Psi(X_\theta, Y_\theta)$.

Figure 8: Marginal distributions $P_\theta(X_\theta)$ obtained by integrating the Wigner function at fixed rotated quadrature X_θ over all conjugate quadratures Y_θ.

A marginal distribution is obtained by fixing X_θ and integrating over all Y_θ :

$$P_\theta(X_\theta) = \int dY_\theta \, W(X_\theta, Y_\theta) \tag{68}$$

and is measurable through homodyne detection. If this is done for a range of different angles θ, then as shown by Risken and Vogel [18], the Wigner function can be obtained from the measured marginals by the Radon transformation familiar from tomographic imaging:

$$W(X,Y) = \frac{1}{4\pi^2} \int_{-\infty}^{\infty} dX_\theta \int_{-\infty}^{\infty} d\xi \, |\xi| \int_0^{\pi} d\theta \, P_\theta(X_\theta) \; \mathrm{e}^{i\xi\,(X_\theta - X\cos\theta - Y\sin\theta)} \; . \tag{69}$$

Raymer and his colleagues at the University of Oregon [19] have shown in a remarkable series of experiments using this "optical tomography" technique how the Wigner functions for various field states can be reconstructed, including a squeezed state generated by a travelling-wave optical parametric oscillator. The group at the University of Konstanz [20] have used tomography to reconstruct the properties of squeezed light; in particular, they have observed that only even photon numbers are found in a squeezed vacuum.

Figure 9: Generation of two output parts by a beam–splitter for joint measurements of position and momentum (or of conjugate quadratures X and Y

2.5 Joint Measurements of p, q in Phase Space

The lack of commutability of momentum and position leads to difficulties in the phase–space description of field modes in quantum optics, as we have seen. What happens if we try to make joint measurements of p and q? Consider the scheme shown in Fig. 9 in which a beam–splitter is used to generate two output modes, such that one may be used to measure q and one to measure p. The difficulties with this kind of joint measurement scheme stems from the unused input port: vacuum noise injected from this port introduces excess noise of the kind considered many years ago by Arthurs and Kelly [21] and reviewed (from the quantum optics perspective) by Leonhardt and Paul [22]. What permits the simultaneous measurement of (p, q) is in fact the unused port shown above in Fig. 9: the output mode variables actually commute (even though the input system variables do not) as they represent system *plus* meter variables; because of the unused port, we can read out the q-variable of one output and p-variable of the other output mode. These commute and can therefore be read separately without adding extra noise beyond that represented by the beam–splitter which superposes the system and the meter variables to generate the two output modes.

When discussing the noise characteristics of an optical field, it is helpful to have some way to compare the system state with that of a reference state (some-

times referred to as a quantum ruler) [23], and to employ Popper's concept of "propensity" [24]. The propensity P_r describes the "dispositional properties to take up certain states", or the tendency of the measured object described by the systems density operator $\hat{\rho}_s$ to take up certain states prescribed by a measuring device (or filter) described by a projection operator $P_{\Phi_f} = |\Phi_f\rangle\langle\Phi_f|$. In comparing system and meter states, one normally employs the probability $Tr(\hat{\rho}_s P_{\Phi_f})$. But imagine tuning the filter, or quantum ruler in phase space: the filter projection operator can be tuned by the action of some unitary transformation U_g by varying some parameter g in the filter:

$$P_{\Phi_f} \longrightarrow U_g^\dagger |\Phi_f\rangle\langle\Phi_f| U_g = P_{\Phi_f}(g) \tag{70}$$

For example, the filter states can be displaced in phase space by the operator

$$U(q,p) = exp(iq\hat{p}/\hbar + i\hat{q}p/\hbar). \tag{71}$$

The propensity can then be written as:

$$\begin{aligned} P_r &= \text{const.} Tr(\hat{\rho}_s P_{\Phi_f}) & (72)\\ &= \text{const.} Tr(\hat{\rho}_s \hat{U}_g^\dagger |\Phi_f\rangle\langle\Phi_f| \hat{U}_g) & (73) \end{aligned}$$

so that we may probe $\hat{\rho}_s$ by moving the filter around to sample all attributes 'g'. For the case of displacements,

$$P_r(q,p) = \frac{1}{2\pi\hbar} Tr(\hat{\rho}_s \hat{U}_g^\dagger(q,p) |\Phi_f\rangle\langle\Phi_f| \hat{U}_g(q,p)) \tag{74}$$

and if the system is prepared in the pure state $\hat{\rho} = |\Psi_f\rangle\langle\Psi_f|$, then

$$\begin{aligned} P_r(q,p) &= \left| \int dx e^{-ipx/\hbar} \Phi_f^*(q+x) \Psi_s(x) \right|^2 & (75)\\ &= \frac{1}{(2\pi\hbar)} \int dq dp W_\Psi(q+q', p+p') W_\Phi(q', p') & (76) \end{aligned}$$

In other words the propensity is given by the convolution of system and quantum ruler Wigner functions. In terms of the Glauber displacement operator $\hat{D}(q,p)$, this may be written as

$$P_{\Psi\Phi} = P_r(q,p) = |\langle\Psi|\hat{D}(q,p)|\Phi\rangle|^2 \tag{77}$$

which shows clearly that the propensity (as distinct from the Wigner function) is always positive. The ruler states act as a smoothing in this convolution process.

Now let us return to the problem of joint measurement of q and p. If the quantum ruler is prepared in the vacuum state $|\Phi\rangle = |0\rangle$

$$\begin{aligned} P_{\Psi\Phi} &= |\langle 0|\hat{D}^\dagger(q,p) \hat{\rho}_\Psi \hat{D}(q,p)|0\rangle|^2 & (78)\\ &= Q_\Psi(q,p) & (79) \end{aligned}$$

Figure 10: 8–port homodyne set–up for joint measurements in phase–space

where $Q_\Psi(q,p)$ is the Husini Q–function. The smoothing implicit in the convolution of the ruler and system states makes the propensity a most useful concept [25].

One way of realizing this optional phase–space measurement is to use the 8–port homodyne device shown in Fig. 10 in which a beam–splitter generates two output fields, each of which is used in a balanced homodyne measurement, one for q, the other for p. Of course what is measured is the system coordinates *plus* the meter (or quantum ruler) noise. The outputs for (q,p) can be fed to an oscilloscope to display directly the Husimi Q–function of the system.

In ordinary homodyne detection, the fields and photon number counts can be easily found [8] from the usual beam–splitter transformation from inputs $\hat{a}_L$ (for local oscillator) and $\hat{a}$ to output modes $\hat{d}_1, \hat{d}_2$ as

$$\begin{pmatrix} \hat{d}_1 \\ \hat{d}_2 \end{pmatrix} = \begin{pmatrix} r & t \\ t & r \end{pmatrix} \begin{pmatrix} \hat{a}_L \\ \hat{a} \end{pmatrix}$$

where the amplitude reflection and transmission coefficients are denote by r and

t. Unitarity demands that

$$|r|^2 + |t|^2 = 1, \tag{80}$$
$$t^* r + r^* t = 0. \tag{81}$$

In ordinary homodyne detection, $|r|^2 \ll |t|^2$, but in balanced homodyne detection $|r| = |t| = 1/\sqrt{2}$. In ordinary homodyne detection the the measured signal is determined by the operator.

$$\hat{d}_1^\dagger \hat{d}_1 = |r|^2 \hat{a}_L^\dagger \hat{a}_L + t^* r \hat{a}_L^\dagger \hat{a}_L + r^* t \hat{a}_L^\dagger \hat{a}_L + |t|^2 \hat{a}^\dagger \hat{a}. \tag{82}$$

If the local oscillator field is prepared in coherent state $|\alpha\rangle_L$, then,

$$\langle \hat{n}_1 \rangle = \langle \hat{d}_1^\dagger \hat{d}_1 \rangle = |r|^2 |\alpha_L|^2 + 2|t||r||\alpha_L| \langle E(\chi) \rangle + |t|^2 \langle \hat{a}^\dagger \hat{a} \rangle \tag{83}$$

where as before $\hat{E}(\chi) = \frac{1}{2}[\exp(i\chi)\hat{a}^\dagger + \exp(-i\chi)\hat{a}]$ and

$$\chi = \arg r - \arg t + \phi_L \tag{84}$$
$$= \frac{\pi}{2} + \phi_L. \tag{85}$$

In ordinary homodyne detection, the strong local oscillator allows us to write the detected photon number approximately as

$$\langle \hat{n}_1 \rangle \cong |r|^2 |\alpha_L|^2 + 2|t||r||\alpha_L| \langle E(\chi) \rangle \tag{86}$$

and the photon number variance as

$$\langle (\Delta n_1)^2 \rangle = |r|^2 |\alpha_L|^2 [|r|^2 + 4|t|^2 |\langle (\Delta E(\chi))^2 \rangle] \tag{87}$$

Of course in practice the photodetectors have a finite quantum efficiency η. This can be modelled [26] by considering the finite efficiency detector to be equivalent to a perfect photodetector preceded by a beam–splitter which transmits only a fraction $\sqrt{\eta}$ of the incident amplitude. The annihilation operator at the detector can be written as

$$\hat{d} = \sqrt{\eta} a + \sqrt{1-\eta} a_v \tag{88}$$

where a_v represents the unavoidable admixture of vacuum field from the other input to the beam–splitter. The field represented by $\hat{d}$ is then assumed to be detected with unit efficiency. Then

$$\langle n \rangle = \eta \langle \hat{a}^\dagger \hat{a} \rangle \tag{89}$$

and

$$\langle \hat{d}^\dagger \hat{d}^\dagger \hat{d} \hat{d} \rangle = \eta^2 \langle \hat{a}^\dagger \hat{a}^\dagger \hat{a} \hat{a} \rangle = \eta^2 \langle \hat{n}(\hat{n} - 1) \rangle. \tag{90}$$

In this way we see (for single mode input where we are not concerned with counting times T) that the *photocount* mean and variance are

$$\begin{aligned} \langle \hat{m} \rangle &= \eta \langle \hat{n} \rangle, & (91) \\ \langle (\Delta m)^2 \rangle &= \eta^2 \langle (\Delta n)^2 \rangle + \eta(1-\eta)\langle \hat{n} \rangle & (92) \end{aligned}$$

Here the 'n"s are really the photon flux in quanta per unit time multiplied by the integration time T. So for the ordinary homodyne detection process, we can write (after subtracting the large local oscillator contribution) the mean photocount as

$$\langle \hat{m} \rangle = 2\eta |t||r||\alpha_L| \langle E(\chi) \rangle \tag{93}$$

and its variance as

$$\langle (\Delta m)^2 \rangle \cong \eta |r|^2 |\alpha_L|^2 \{ 1 + \eta |t|^2 [4 \langle (\Delta E(\chi))^2 \rangle - 1] \}. \tag{94}$$

The first "1" term in the above is the shot noise contribution, and the remaining term vanishes for a coherent signal input. If the input signal is squeezed, with $\langle (\Delta E(\chi))^2 \rangle < 1/4$ for some phase angle χ, then the photocount variance is reduced *below* the shot–noise limit.

For *balanced* homodyne detection, the difference in the two photodetector counts is measured: the relevant quantity is

$$\hat{d}_1^\dagger \hat{d}_1 - \hat{d}_2 \hat{d}_2^\dagger = i(\hat{a}^\dagger \hat{a}_l - \hat{a}_l^\dagger \hat{a}) \tag{95}$$

and the mean difference photon number is

$$\langle n_{12} \rangle = \langle \hat{d}_1^\dagger \hat{d}_1 - \hat{d}_2 \hat{d}_2^\dagger \rangle = 2|\alpha_L| \langle E(\chi) \rangle \tag{96}$$

with variance (again assuming $|\alpha_L|$ is large)

$$\langle (\Delta n_{12})^2 \rangle = 4|\alpha_L|^2 \langle (\Delta E(\chi))^2 \rangle \tag{97}$$

so that the balancing removes the local oscillator contribution to the noise. For the *photocounts*, taking into account the finite efficiency we find

$$\begin{aligned} \langle m_{12} \rangle &= 2\eta |\alpha_L| \langle E(\chi) \rangle & (98) \\ \langle (\Delta m_{12})^2 \rangle &= \eta |\alpha_L|^2 \{ 1 + \eta [4 \langle (\Delta E(\chi))^2 \rangle - 1] \}. & (99) \end{aligned}$$

If we now use these (4-port) homodyne results to describe the 8–port joint measurement scheme, then we find for the difference photocounts in the 1–2 and 3–4 detectors

$$\begin{aligned} \langle m_{12} \rangle &= \eta |\alpha_L| \langle E(\chi + \frac{\pi}{2}) \rangle & (100) \\ \langle m_{34} \rangle &= \eta |\alpha_L| \langle E(\chi) \rangle & (101) \end{aligned}$$

so that, as claimed, the 8–port device measures the two quadrature components of the input field, with phase determined by χ. A suitable adjustment of this allows us to measure X (or q) in the 1–2 pair, and Y in the 3–4 pair. The photocount difference variances are [8]

$$\langle(\Delta m_{12})^2\rangle = \frac{1}{4}\eta|\alpha_L|^2\{2+\eta[4\langle(\Delta E(\chi+\frac{\pi}{2}))^2\rangle-1]\} \quad (102)$$

$$\langle(\Delta m_{34})^2\rangle = \frac{1}{4}\eta|\alpha_L|^2\{2+\eta[4\langle(\Delta E(\chi))^2\rangle-1]\} \quad (103)$$

If we compare these 8–port variances with the usual 4–port homodyne, we see the "1" factor in the curly brackets has been replaced by "2". This is because the photocount variances are no longer determined solely by the input ((system) variances alone (even in the case of perfect detectors). The additional contributions to the photocount fluctuations in the 8–port device can be traced back to the entrance of vacuum fluctuations in the two unused parts. The additional noise [8] is precisely the Arthurs–Kelly excess noise which takes us from the Wigner function of the input to the smoother, broader, noisier Husimi Q–function measured in the joint–detection of the conjugate variables. Loudon [27] has discussed how the concept of "detector squeezed states" [28] can be employed for both 4–port and 8–port detectors. The experimental realization of this 8–port homodyne joint measurement of q, p (or equivalently of the quadratures X and Y), was undertaken by Walker and Carroll [29], where the joint measurement results of measuring the quadratures X and Y for a helium–neon laser output field were displayed on an oscilloscope screen. As far as I know, such measurements have not been attempted for nonclassical fields.

If our system of interest is prepared in a coherent state $|\psi\rangle = |\alpha\rangle$, then of course this is a minimum uncertainty state with $\langle(\Delta\hat{q})^2\rangle_\psi = \langle\psi|(\Delta\hat{q})^2|\psi\rangle = \hbar/2 = \langle(\Delta\hat{p})^2\rangle$. But what of the joint properties of the system and the ruler? We can define the joint *marginals* from the propensities through

$$P_{\psi\phi}(q) = \frac{1}{\lambda\sqrt{(2\pi\hbar)}}\int dp P_{\psi\phi}(p,q) \quad (104)$$

$$P_{\psi\phi}(p) = \frac{\lambda}{\sqrt{(2\pi\hbar)}}\int dq P_{\psi\phi}(p,q). \quad (105)$$

We note these carry information about system *and* ruler. For example, consider the expectation value of the position operator

$$\langle\hat{q}\rangle_{\psi\phi} = \frac{\lambda}{\sqrt{(2\pi\hbar)}}\int dq q P_{\psi\phi}(q) \quad (106)$$

$$= \langle\psi|\hat{q}|\psi\rangle - \langle\phi|\hat{q}|\phi\rangle. \quad (107)$$

Similarly, for the momentum operator we find

$$\langle\hat{p}\rangle_{\psi\phi} = \langle\psi|\hat{p}|\psi\rangle - \langle\phi|\hat{p}|\phi\rangle \quad (108)$$

so these averages give the *relative* "distance" of the detected state with respect to the reference fixed by the quantum ruler or filter state. We can therefore define the *operational* variances :

$$\Sigma^2_{\psi\phi}(q) = \langle \hat{q}^2 \rangle_{\psi\phi} - \langle \hat{q} \rangle^2_{\psi\phi} \tag{109}$$

$$= \langle (\Delta \hat{q})^2 \rangle_{\psi} + \langle (\Delta \hat{q})^2 \rangle_{\phi} \tag{110}$$

$$\Sigma^2_{\psi\phi}(p) = \langle (\Delta \hat{p})^2 \rangle_{\psi} + \langle (\Delta \hat{p})^2 \rangle_{\phi} \tag{111}$$

which directly exhibit the *two* sources of measured quantum fluctuations: those from the system *and* those from the filter. The product of the two is:

$$\Sigma^2_{\psi\phi}(q)\Sigma^2_{\psi\phi}(p) \geq \hbar^2 \tag{112}$$

which is a factor of 4 greater than those of the system alone. This additional noise is precisely of the kind described by Arthurs and Kelly. To illustrate this, consider the case where the system is prepared in the M.U.S. squeezed state $|\eta\rangle$ (with η within $[-1, 1]$). Then

$$\langle (\Delta \hat{q})^2 \rangle_{\psi} = \frac{\hbar}{2}\frac{1-\eta}{1+\eta} = \hbar\sigma^2_q(\psi) \geq \frac{\hbar}{2}; \tag{113}$$

$$\langle (\Delta \hat{p})^2 \rangle_{\psi} = \frac{\hbar}{2}\frac{1+\eta}{1-\eta} = \hbar\sigma^2_p(\psi) < \frac{\hbar}{2}. \tag{114}$$

If the quantum ruler is prepared in a coherent state (or the vacuum as in fig(10)) $|\phi\rangle = |\beta\rangle$, then

$$\langle (\Delta \hat{q})^2 \rangle_{\psi} = \frac{\hbar}{2} = \langle (\Delta \hat{p})^2 \rangle_{\psi} \tag{115}$$

but the operational variances are

$$\Sigma^2_{\psi\phi}(q) = \frac{\hbar}{1-\eta} \tag{116}$$

$$\Sigma^2_{\psi\phi}(p) = \frac{\hbar}{1+\eta} \tag{117}$$

and the product of the operational variances

$$\Sigma^2_{\psi\phi}(q)\Sigma^2_{\psi\phi}(p) = \frac{\hbar^2}{1-\eta^2} > \hbar^2 \tag{118}$$

is definitely *not* of M.U.S. kind. For the simpler case of the system prepared in a coherent state, $\Sigma^2_{\psi\phi}(q) = \hbar = \Sigma^2_{\psi\phi}(p)$ and the product is $\hbar^2$, again exhibiting Arthurs–Kelly excess noise even for these coherent field inputs.

2.6 Phase–Space Sampling Entropies

Unless the states are Gaussian, we need more than the variances to characterize the fluctuations. One approach is to employ entropies. The most commonly used is the von Neumann entropy [30]

$$S_{\hat{\rho}} = k_B Tr\{\hat{\rho}_\psi \ln \hat{\rho}_\psi\} \tag{119}$$

where k_B is Boltzmann's constant but for *pure* states, this entropy is zero. It would be useful to find an entropy measure which contains information about not just the deviation from a pure state (the classical, mixed state fluctuation) but also about the quantum uncertainties. One approach [31] employs the operational phase–space or propensity distribution to define a phase–space *sampling* entropy through

$$S_{\psi\phi}(q,p) = \frac{-k_B}{\sqrt{(2\pi\hbar)}} \int dq dp\, P_{\psi\phi}(p,q) \ln P_{\psi\phi}(p,q)\,. \tag{120}$$

As we shall see, this is analogous to Boltzmann's entropy

$$S_B = k_B \ln W \tag{121}$$

where W is the number of microstates needed to realize a given macrostate. The sampling entropy $S_{\psi\phi}(p,q)$ may be interpreted in terms of the number of quantum ruler states $|\phi\rangle$ which sample the system state $|\psi\rangle$. If we could violate quantum mechanics with an ultra–sharp (and entirely unphysical) filter with a filter Wigner function

$$W_\phi(q,p) \sim \delta(p-p')\delta(q-q') \tag{122}$$

then you could attempt to define an entropy in terms of the system Wigner function $W_\psi(q,p)$ alone. Of course, this is impossible: filters *cannot* be prepared in these artificially sharp states, which is just as well, for the system Wigner function could be negative in some region of phase–space rendering the logarithm impossible. Real filters introduce excess noise as the price we need to pay to make joint measurements. The joint phase–space marginals can be used to define entropies for the marginals

$$S^{(q)}_{\psi\phi} = \frac{-\lambda k_B}{\sqrt{(2\pi\hbar)}} \int dq\, P_{\psi\phi}(q) \ln P_{\psi\phi}(q) \tag{123}$$

$$S^{(p)}_{\psi\phi} = \frac{-k_B}{\sqrt{(2\lambda\pi\hbar)}} \int dp\, P_{\psi\phi}(p) \ln P_{\psi\phi}(p) \tag{124}$$

describing the fluctuations in the measurement values of p or q provided the ruler was prepared in the state $|\phi\rangle$. For example, if the ruler is prepared in an *eigenstate* of the measured observable (say $\hat{q}$, then $|\psi\rangle = |q\rangle$ and

$$P_{\psi\phi}(q) = |\langle q|\psi\rangle|^2 \tag{125}$$

and $P^{(q)}_{\psi\phi}$ is the *Shannon* entropy for measurements of the single observable $\hat{q}$. The fluctuations associated with the ruler are then zero (for *this* observable), $\langle(\Delta\hat{q})^2\rangle_{\phi=q} = 0$, so $\Sigma_{\psi,\phi=q}(q) = \langle(\Delta\hat{q})^2\rangle_\psi$, the system "intrinsic fluctuations". Of course there are infinite fluctuations in the un–read conjugate variable p.

2.7 Mutual Information and Entropic Uncertainty

Consider two random variables, A defined on the stochastic object $x_i (i = 1 \ldots n)$ and B, defined on the stochastic object $y_i (i = 1 \ldots n)$, with probabilities $P^{(A)})x_i)$ and $P^{(B)})y_j)$ and appropriate marginals

$$P^{(A)}(x_i) = \sum_j P^{(A,B)}(x_i, y_j) \tag{126}$$

$$P^{(B)}(y_j) = \sum_i P^{(A,B)}(x_i, y_j). \tag{127}$$

Then the Kolmogororoff–Shannon Mutual Information $I^{(A,B)}$ between the random variables A and B is defined as

$$I(A,B) \equiv k_B \sum_{i,j} P^{(A,B)}(x_i, y_j) \ln\{\frac{P^{(A,B)}(x_i, y_j)}{P^{(A)}(x_i) P^{(B)}(y_j)}\} \tag{128}$$

and gives a measure of the information contained for example in the random variable A about the variable B (and vice–versa). If the two variables are statistically uncorrelated, $I^{(A,B)} = 0$, but otherwise $I^{(A,B)} \geq 0$. We can employ the Mutual Information for the phase–space measurements

$$I^{(q,p)}_{\psi,\phi} \equiv \frac{k_B}{2\pi\hbar} \int P_{(\psi\phi)}(q,p) \ln\{\frac{P_{\psi\phi}(q,p)}{P_{\psi\phi}(q) P_{\psi\phi}(p)}\} \tag{129}$$

to describe the amount of information contained in the measurement of position (momentum) of the system in state $|\psi\rangle$ about the momentum (position) provided the measurement is performed with the quantum ruler prepared in state $|\phi\rangle$. We see that the entropies satisfy the inequality

$$I^{(q,p)}_{\psi,\phi} = S^{(q)}_{\psi\phi} + S^{(p)}_{\psi\phi} - S^{(q,p)}_{\psi\phi} \tag{130}$$

which is reminiscent of the Araki–Lieb inequality for entangled systems [32]. We can therefore construct an entropic uncertainty relation (EUR)

$$S^{(q)}_{\psi\phi} + S^{(p)}_{\psi\phi} \geq S^{(q,p)}_{\psi\phi}. \tag{131}$$

If we return to the sampling entropy

$$S_{\psi\phi}(q,p) = \frac{-k_B}{\sqrt{(2\pi\hbar)}} \int dq dp P_{\psi\phi}(p,q) \ln P_{\psi\phi}(p,q) \tag{132}$$

with

$$P_{\psi\phi}(p,q) = \frac{1}{\sqrt{(2\pi\hbar)}} \int dq'dp'\, W_\psi(q+q', p+p') W_\phi(q',p') \tag{133}$$

and prepare the filter in a coherent state $|\alpha\rangle$ then the sampling entropy is the *Wehrl* entropy $S_W(\alpha)$ [33]

$$S_{\psi,\alpha} = S_W(\alpha). \tag{134}$$

For this coherent state quantum ruler, the propensity $P_{\psi\phi}(p,q)$ is just the Husimi Q–function for the system state, and

$$S_W(\alpha) = \frac{-k_B}{\sqrt{(2\pi\hbar)}} \int dqdp\, Q_\psi(\alpha) \ln Q_\psi(\alpha). \tag{135}$$

If the system has been prepared in a single coherent state itself, then its Q–function is the Gaussian centered on the mean values $\bar{q}, \bar{p}$,

$$Q_\psi(p,q) = \frac{1}{\Sigma_p \Sigma_q} \exp\{-\frac{1}{2\hbar}\frac{(q-\bar{q})^2}{\Sigma_q^2} - \frac{1}{2\hbar}\frac{(p-\bar{p})^2}{\Sigma_p^2}\} \tag{136}$$

with widths

$$\Sigma_q^2 = \frac{1}{2} + \sigma_q^2, \tag{137}$$

$$\Sigma_p^2 = \frac{1}{2} + \sigma_p^2 \tag{138}$$

then the product $\Sigma_q\Sigma_p = A$ is the area (in units of $2\pi\hbar$) of phase–space covered by the error contour of the Q–function at $(1/e)$ of its maximum value, so that in general,

$$S_{\psi,\alpha}^{(q,p)} \cong k_B + k_B \ln \Sigma_q\Sigma_p\,. \tag{139}$$

For a single coherent state, $A = \Sigma_q\Sigma_p = 1$, $\ln A = 0$ and the Wehrl entropy achieves its *minimum* value of k_B. For a state made up of N well–separated coherent states (either a superposition or a mixture), then $A = N$ and

$$S_W(\alpha) \cong k_B + k_B \ln N. \tag{140}$$

The first term derives from the fact that our quantum ruler coherent states are not really orthogonal, whereas the second is essentially the Boltzmann contribution from the N well–separated (and therefore approximately orthogonal) microstate components of the system. Orlowski [34] has calculated the Wehrl entropy for a number of states of interest in quantum optics, including squeezed states, number states, phase–diffused coherent states and thermal states. Bužek et al [31] have examined various superposition states including a Schrödinger cat superposition of coherent states.

2.8 Building Nonclassical States by Quantum Interference

We turn next to the question of how nonclassical states can be created in terms of component states which may be Fock states or coherent states. We can construct nonclassical states (or any other states) as superpositions of Fock states $|n\rangle$ as

$$|\Psi\rangle = \sum_n c_n |n\rangle . \tag{141}$$

The Wigner functions for each Fock state component are given by Laguerre polynomials. These interfere to generate the superposition of interest. The Fock state components are radially symmetric, and tile phase-space in annulae. As an alternative basis, we can construct our state from superpositions of coherent states

$$|\Psi\rangle = \sum_\alpha c(\alpha) |\alpha\rangle \tag{142}$$

which tile phase-space in circular patches. The coherent states, of course, form an over-complete set and are not orthogonal but form a perfectly respectable basis set. A finite number of states $|\alpha\rangle$ may be used for the construction, or a continuous superposition may be employed in which case the sum in eq. (142) becomes an integral. The particular basis which we employ is not entirely a matter of taste as we shall see.

The simplest example of a nonclassical superposition is the superposition of the vacuum and one photon state [35] so that

$$|\Psi\rangle = c_0 |0\rangle + c_1 |1\rangle . \tag{143}$$

This state can exhibit squeezing (in a sense it is the simplest squeezed state), with quadrature variances

$$(\Delta X)^2 = \frac{1}{4} + \frac{1}{2} \left(|c_1|^2 - 2 |c_1|^2 \cos^2 \Delta\phi + 2 |c_1|^4 \cos^2 \Delta\phi \right) \tag{144}$$

$$(\Delta Y)^2 = \frac{1}{4} + \frac{1}{2} \left(|c_1|^2 - 2 |c_1|^2 \sin^2 \Delta\phi + 2 |c_1|^4 \sin^2 \Delta\phi \right) \tag{145}$$

where $\Delta\phi$ is the relative phase between c_0 and c_1. It is obvious that this state is *not* a minimum uncertainty state (M.U.S.). We find the mean value of the quadrature is non-zero, reflecting the coherence in the superposition, and for the variances we find

$$\begin{aligned} (\Delta X)^2_{\Delta\phi=0,\pi} &= (\Delta Y)^2_{\Delta\phi=\pi/2,3\pi/2} \\ &= \frac{1}{4} + |c_1|^2 \left(|c_1|^2 - \frac{1}{2} \right) \end{aligned} \tag{146}$$

with $(\Delta X)^2$ being reduced below its coherent state (or vacuum state) value of $(1/4)$ by a maximum of $(1/16)$ when $|c_1| = 1/2$. The Wigner function for the

Figure 11: Wigner function for a superposition of the vacuum and one photon state, eq. (143).

state given by eq. (143) is shown in Fig. 11, where both negativity *and* squeezing are visible. The squeezing is not of M.U.S. form.

The superposition of the vacuum and the two photon state

$$|\Psi\rangle = c_0\,|0\rangle + c_2\,|2\rangle \tag{147}$$

generates rather more squeezing, although this time the mean values of the quadratures are zero, reflecting the two-photon coherence. We find for the quadrature variances,

$$(\Delta X)^2 = \frac{1}{4}\left(1 + 4\,|c_2|^2 + 2\sqrt{2}\,|c_2|\,(1-|c_2|^2)^{\frac{1}{2}}\,\cos\Delta\phi\right), \tag{148}$$

$$(\Delta Y)^2 = \frac{1}{4}\left(1 + 4\,|c_2|^2 - 2\sqrt{2}\,|c_2|\,(1-|c_2|^2)^{\frac{1}{2}}\,\cos\Delta\phi\right), \tag{149}$$

so that again the squeezing is not of minimum uncertainty form, but is more pronounced than the one-photon superposition: at $|c_2|^2 = (1/2)-(1/\sqrt{6})$ we find 45% maximum squeezing below the vacuum value of the quadrature variance. The Wigner function for this two-photon superposition is shown in Fig. 12. This process of squeezing by superposition is improved by superposing *all* of the even number states as in the classic squeezed vacuum [8], although the complicated interference between the infinite number of Fock components actually reduces to a simple Gaussian squeezed state, which *is* of M.U.S. form.

More interesting nonclassical states can be generated by superposing coherent states $|\alpha\rangle$, and the "Schrödinger cat state"

$$|\Psi\rangle = \frac{1}{N_+(\alpha)}\,\left\{|\alpha\rangle\;+\;|-\alpha\rangle\right\}\;, \tag{150}$$

where $N_+(\alpha)$ is a normalization factor, is the best studied example [36]. It is also interesting to examine the nature of the Wigner function for the state formed by a superposition of a number of coherent states as that number N increases, whilst maintaining each component on a ring of radius R [37]. We write for this N component superposition on a ring of radius R in phase-space

$$|\Psi\rangle = \frac{1}{W}\,\sum_{j=0}^{N-1}\,\exp\left\{-\frac{2\pi i}{N}\,Kj\right\}\,|R\,\exp\left(2\pi i K j/N\right)\rangle \tag{151}$$

where K is something we will call the "target" number, for reasons which will become apparent very quickly and W is a normalization factor. For $N = 2$, we see a Gaussian hump for each constituent state, together with fringes whose period scales inversely with the separation between the components in phase-space: the more macroscopic the superposition, the more rapid are the fringe oscillations. For $N = 4$ we see four constituent "humps" together with complicated interference structures between them. When the number of states is increased

Figure 12: Wigner function for a superposition of the vacuum and two-photon state, eq. (147).

Figure 13: Dependence of the number uncertainty Δn of the superposition of N coherent states on a ring of radius $R = 3$ in phase-space, with a phase-factor $\exp\{-2\pi i K j/N\}$ for each component j to ensure a target Fock state $|K\rangle$ is generated as N increases. Here $K = 4$, so the initial radius is not optimal. Nevertheless, after complicated interference at intermediate N with large fluctuations, we see a sharp reduction in Δn.

so that the individual components nearly, but not quite, fill the circumference of the ring we see a sequence of interference structures, large amounts of negativity in the Wigner functions and large fluctuations in the photon number. But when the number of coherent states is sufficiently increased to cover entirely the circumference of the ring (of radius R), then a dramatic change occurs [37] with a collapse of the number variance as the superposition approaches ... a number state! This is seen for increasing N in Fig. 13. A continuous superposition of coherent states on a ring with an appropriate choice of phases is in fact a representation of a Fock state $|n\rangle$ [36, 38]

$$|n\rangle = \frac{\mathrm{e}^{|\alpha|^2/2}\sqrt{n!}}{2\pi|\alpha|^n} \int_0^{2\pi} \mathrm{d}\phi \; \mathrm{e}^{-in\phi} \; \left||\alpha|\,\mathrm{e}^{i\phi}\right\rangle \; . \tag{152}$$

It is amusing that coherent states, the most classical of all states, can be used to build Fock states using quantum interference. We have discussed elsewhere

[39] how a sequence of conditional measurements in cavity QED may be used to realize the progression from coherent state to Fock state.

If coherent states are continuously superposed on a line

$$|\Psi\rangle = C_F \int_{-\infty}^{\infty} F(\alpha, s)|\alpha\rangle \, \mathrm{d}\alpha \, , \tag{153}$$

with $F(\alpha, s)$ chosen to be a Gaussian function of α along the line but centred on the origin, so that α is here taken as real, it is easy to demonstrate that the resultant state is a sum over even Fock states only and is in fact the squeezed vacuum [38, 40]: to do so we first write the coherent state $|\alpha\rangle$ in a Fock basis as a Poisson superposition

$$|\alpha\rangle = \sum_{m=0}^{\infty} \frac{\alpha^m}{\sqrt{m!}} \, \mathrm{e}^{-\frac{1}{2}\alpha^2} |m\rangle \tag{154}$$

and take as an explicit form of $F(\alpha, s)$ the Gaussian centred on the origin

$$F(\alpha, s) = \exp\{-\frac{(1-s)}{2s} \, \alpha^2\} \tag{155}$$

so that $C_F^{-2} = \pi \, (1-s^2)^{\frac{1}{2}} / \, 2s$, then

$$|\Psi\rangle = C_F \int_{-\infty}^{\infty} F(\alpha, s) \, \mathrm{e}^{-\frac{1}{2}\alpha^2} \sum_m \frac{\alpha^m}{\sqrt{m!}} |m\rangle \, d\alpha \, . \tag{156}$$

Then if we interchange the order of integration and summation we find

$$|\Psi\rangle = C_F \sum_{m=0}^{\infty} \frac{1}{\sqrt{m!}} |m\rangle \int_{-\infty}^{\infty} d\alpha \, \alpha^m \, \mathrm{e}^{-\alpha^2/2s} \tag{157}$$

and perform the Gaussian integral, we find the result is the squeezed vacuum

$$\begin{aligned} |\Psi\rangle &= (1-s^2)^{\frac{1}{4}} \sum_{m=0}^{\infty} \frac{\sqrt{2m!}}{2^n \, n!} \, s^n \, |2n\rangle \\ &= \hat{S}(s) \, |0\rangle \end{aligned} \tag{158}$$

where $\hat{S}(s)$ is the quadratic squeeze operator [8]. For this state, the quadratic variances are

$$(\Delta X)^2 = \frac{1}{4} \left(\frac{1+s}{1-s} \right) \tag{159}$$

$$(\Delta Y)^2 = \frac{1}{4} \left(\frac{1-s}{1+s} \right) \tag{160}$$

so that this state *is* of M.U.S. form.

3 Dissipation Versus Coherent Evolution: Decoherence

So far, we have discussed our superposition states as if they were entirely isolated: in reality, all systems are in contact to some extent with an external world which we can model as an infinite reservoir, or heat-bath. The system dissipates both coherence and energy irreversibly upon interaction with such a reservoir, and in turn the reservoir feeds back Langevin noise into the microsystem. If the system and reservoirs are described by Hamiltonians H_R and H_S, and the interaction between them denoted $\hat{V}$, then the total system-plus-reservoir density matrix evolves in the interaction picture as

$$\dot{\rho} = -\frac{i}{\hbar}\,[\hat{V}, \rho]\,. \tag{161}$$

Initially the system and the reservoir are uncorrelated, so the initial density operator factorises into a product of subsystem reduced density operators

$$\rho(0) = \rho_S(0) \otimes \rho_R(0)\,. \tag{162}$$

We may formally integrate the Liouville equation of motion eq. (161) and iterate, to give

$$\rho(t) = \rho(0) - \frac{i}{\hbar}\int_0^t dt_1[\hat{V}(t_1), \rho(t_1)]\,. \tag{163}$$

If we iterate one more time, and trace over the reservoir states assuming

(i) $\mathrm{Tr}_R(\hat{V}(t)\rho_R) = 0$
(ii) $\hat{V}$ is "weak"

then we find

$$\dot{\rho}_S = (-\frac{1}{\hbar})^2 \int_0^t dt_1\, \mathrm{Tr}_R[\hat{V}(t), [\hat{V}(t_1), \rho_R \otimes \rho_S(0)]]\,. \tag{164}$$

If the system of interest is a harmonic oscillator described by annihilation $\hat{a}$ and creation operators $\hat{a}^\dagger$, and is coupled to a bath of oscillators described by $\hat{b}_j$, $\hat{b}_j^\dagger$, then [41]

$$\hat{V}(t) = \hbar\,\hat{a}^\dagger\,\hat{\Gamma}(t)\,\mathrm{e}^{i\omega_0 t} + \hbar\,\hat{a}\,\hat{\Gamma}^\dagger(t)\,\mathrm{e}^{-i\omega_0 t}$$

where the reservoir operators are

$$\hat{\Gamma}(t) = \sum_j g_j \hat{b}_j\,\mathrm{e}^{-i\omega_j t}\,, \qquad [\hat{b}_j, \hat{b}_k^\dagger] = \delta_{jk} \tag{165}$$

and ω_0 is the resonance frequency of the system oscillator. The integrals in eq. (164) can then be expressed as

$$I = \int_0^t dt_1 \langle \hat{\Gamma}(t)\hat{\Gamma}^\dagger(t_1)\rangle\,\mathrm{e}^{i\omega_0\,(t-t_1)} \tag{166}$$

which can be broken into real (widths) and imaginary (shift) parts as

$$I \to \frac{\gamma}{2}\,(N(\omega_0)+1) - i\Delta \tag{167}$$

(for details see [3, 41]), where $N(\omega_0)$ is given by the mean number of reservoir excitations at frequency ω_0 :

$$2\pi\, N(\omega)\,\delta(\omega-\omega') = \langle \hat{b}^\dagger(\omega)\hat{b}(\omega')\rangle\,. \tag{168}$$

For a normal unsqueezed reservoir, we finally obtain the Born-Markov master equation

$$\begin{aligned}\dot{\rho}_S &= \frac{\gamma}{2}\,(N+1)\,(2\,\hat{a}\rho_S\hat{a}^\dagger - \hat{a}^\dagger\hat{a}\rho_S - \rho_S\hat{a}^\dagger\hat{a}) \\ &\quad + \frac{\gamma}{2}\,N\,(2\,\hat{a}^\dagger\rho_S\hat{a} - \hat{a}\hat{a}^\dagger\rho_S - \rho_S\hat{a}\hat{a}^\dagger)\,.\end{aligned} \tag{169}$$

At zero temperature, $N=0$, so that

$$\dot{\rho}_S = \frac{\gamma}{2}\,(2\hat{a}\rho_S\hat{a}^\dagger - \hat{a}^\dagger\hat{a}\rho_S - \rho_S\hat{a}^\dagger\hat{a})\,. \tag{170}$$

In Fig. 14, we show the Wigner function for a nine-photon Fock state, but including dissipation to a zero-temperature heat-bath, computed from eq. (170) at time $\gamma t = 0.1$. We note that the fringes which were so prominent in Fig. 5 have almost completely disappeared, and the prominent negativity has been much reduced (even though the initial energy is hardly depleted).

The master equation emphasises the evolution of an entire ensemble [3]. Coherences are destroyed at a rate which is proportional to the degree of excitation of the system (much faster than energy decay) as the system relaxes to a statistical mixture of relevant "pointer bases" [4, 42, 43]. For example, a field mode initially prepared in a Fock state relaxes very rapidly to a statistical mixture of Fock states, and the fringing structure in the Wigner function disappears at a rate $\sim n\gamma$. Such an ensemble-averaged approach does not easily address the question of how an individual member of an ensemble evolves in a dissipative environment, even though this issue is accessible to experiment [44]. A number of methods have been developed recently to simulate the evolution of single realizations. One centres on quantum jumps, reflecting the information gained from the detection of decay quanta, and involves a continuous evolution which is randomly interrupted by "instantaneous" jumps as the system state vector is conditioned by the information gained from the register of counts in detection of decay [45, 5].

4 Unravelling the Master Equation

Carmichael [5] has given a precise relationship between the conditioned density operator contingent on a precise sequence of detection events (a "record") and

Figure 14: Wigner function for a field initially prepared in a nine-photon Fock state, after interacting with a zero-temperature reservoir for a time $\gamma t = 0.1$.

the ensemble averaged density operator. He shows for example that if the zero temperature boson damping master equation (eq.(170)) is written in Liouvillian form

$$\frac{\mathrm{d}\rho}{\mathrm{d}t} \;=\; \mathcal{L}\rho \tag{171}$$

and we split the Liouvillian action $\mathcal{L}$ as a sum of two terms, an anticommutator and a "sandwich" term,

$$\begin{aligned} \mathcal{L}\rho &= -\frac{\gamma}{2}\left[\hat{a}^\dagger\hat{a}\;,\;\rho\right]_+ \;+\; \gamma\hat{a}\,\rho\hat{a}^\dagger \\ &= (\mathcal{L}-\mathcal{S})+\mathcal{S} \end{aligned} \tag{172}$$

then we may identify the "sandwich" term $\mathcal{S}$ as a jump operator. Equation (171) can be integrated formally as

$$\begin{aligned} \rho(t) &= \exp\left\{[(\mathcal{L}-\mathcal{S})+\mathcal{S}]\,t\right\}\rho(0) \\ &= \sum_{m=0}^{\infty}\int_0^t \mathrm{d}t_m \int_0^{t_m}\mathrm{d}t_{m-1}\;\ldots\;\int_0^{t_2}\mathrm{d}t_1 \\ &\quad\times\left\{\mathrm{e}^{(\mathcal{L}-\mathcal{S})(t-t_m)}\,\mathcal{S}\,\mathrm{e}^{(\mathcal{L}-\mathcal{S})(t_m-t_{m-1})}\,\mathcal{S}\ldots\mathcal{S}\,\mathrm{e}^{(\mathcal{L}-\mathcal{S})t_1}\rho(0)\right\} \end{aligned} \tag{173}$$

where the quantity in curly brackets in Eq. (173) is labelled $\overline{\rho_c}(t)$ by Carmichael and is the conditioned density operator describing a specific "trajectory" or detection sequence. We can write $\overline{\rho_c}(t)$ in terms of the conditioned pure state projectors

$$\overline{\rho_c}(t) = |\overline{\Psi}_c(t)\rangle\langle\overline{\Psi}_c(t)|\;. \tag{174}$$

The component $\exp[(\mathcal{L}-\mathcal{S})\Delta t]$ propagates $\overline{\rho_c}(t)$ for a time Δt without a decay being recorded: for the conditioned state $|\overline{\Psi}_c(t)\rangle$

$$|\overline{\Psi}_c(t+\Delta t)\rangle \;=\; \exp\left[-iH_{\mathrm{eff}}\Delta t/\hbar\right]\;|\overline{\Psi}_c(t)\rangle \tag{175}$$

where the non-Hermitian effective Hamiltonian

$$H_{\mathrm{eff}} \;=\; H \;-\; i\hbar\frac{\gamma}{2}\hat{a}^\dagger\hat{a} \tag{176}$$

derives from the anticommutator in Eq. (172). Once a decay is registered, the gain in information is responsible for the jump

$$|\overline{\Psi}_c(t)\rangle \longrightarrow \hat{a}\;|\overline{\Psi}_c(t)\rangle\;. \tag{177}$$

The procedure adopted in quantum jump simulations can then be summarized as follows [45]:

1. Determine the current probability of an emission:

$$\Delta P = \gamma\,\Delta t\,\langle\Psi|\hat{a}^\dagger\hat{a}|\Psi\rangle\;. \tag{178}$$

2. Obtain a random number r between zero and one, compare with ΔP and decide on emission as follows:

3. Emit if $r < \Delta P$, so that the system jumps to the renormalized form:

$$|\Psi\rangle \longrightarrow \frac{\hat{a}|\Psi\rangle}{\sqrt{\langle\Psi|\hat{a}^\dagger\hat{a}|\Psi\rangle}}\,. \tag{179}$$

4. Or no emission if $r > \Delta P$, so the system evolves under the influence of the non-Hermitian form

$$|\Psi\rangle \longrightarrow \frac{\{1-(i/\hbar)\,H\Delta t-(\gamma/2)\,\Delta t\,\hat{a}^\dagger\hat{a}\}|\Psi\rangle}{(1-\Delta P)^{\frac{1}{2}}}\,. \tag{180}$$

5. Repeat to obtain an individual trajectory, or history.

6. Average observables over many such trajectories.

To reassure ourselves that this is all true, we note the history splits into two alternatives in a time Δt :

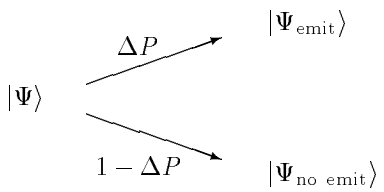

Then in terms of the density matrix, the evolution for a step Δt becomes a sum of the two possible outcomes,

$$\begin{aligned}
|\Psi\rangle\langle\Psi| \;\longrightarrow\; & \Delta P\,|\Psi_{\rm emit}\rangle\langle\Psi_{\rm emit}| \\
& +\,(1-\Delta P)\,|\Psi_{\rm no\ emit}\rangle\langle\Psi_{\rm no\ emit}| \qquad (181)\\
=\; & \gamma\Delta t\,\hat{a}|\Psi\rangle\langle\Psi|\hat{a}^\dagger \\
& +\,\{1-\frac{i}{\hbar}\,H\Delta t-\frac{\gamma}{2}\,\Delta t\,\hat{a}^\dagger\hat{a}\}|\Psi\rangle\langle\Psi|\{1+\frac{i}{\hbar}\,H\Delta t-\frac{\gamma}{2}\,\Delta t\,\hat{a}^\dagger\hat{a}\} \\
\sim\; & |\Psi\rangle\langle\Psi|-\frac{i}{\hbar}\,\Delta t\,[H,|\Psi\rangle\langle\Psi|] \\
& +\,\frac{\gamma}{2}\,\Delta t\,\{2\,\hat{a}|\Psi\rangle\langle\Psi|\hat{a}^\dagger-\hat{a}^\dagger\hat{a}|\Psi\rangle\langle\Psi|-|\Psi\rangle\langle\Psi|\hat{a}^\dagger\hat{a}\} \qquad (182)
\end{aligned}$$

so that

$$\frac{\Delta\rho}{\Delta t}=-\frac{i}{\hbar}\,[H,\rho]+\frac{\gamma}{2}\,\{2\,\hat{a}\rho\hat{a}^\dagger-\hat{a}^\dagger\hat{a}\rho-\rho\hat{a}^\dagger\hat{a}\} \tag{183}$$

Figure 15: Quantum jumps in the decay of a Fock state: evolution of the photon number from an initial value $n =$ due to dissipative coupling. Here the decay rate γ is .

as in the original master equation (171). We see that the form of the Monte-Carlo simulation scheme above is of the Euler form, and as such is a rather crude numerical approach. More accurate methods involve both Runge-Kutta and so-called "higher-order" unravellings or "mini-trajectories". We have addressed this point elsewhere [46].

The quantum jump method applied to an initial Fock state interacting with a zero-temperature heat-bath is particularly simple to describe. The non-Hermitian no-jump evolution is described by

$$H_{\rm eff} = -i\hbar\,\frac{\gamma}{2}\hat{a}^\dagger\hat{a} \tag{184}$$

which does, of course, not change the photon number. On the other hand, a jump from $|n\rangle$ to $|n-1\rangle$ occurs with probability $\gamma\langle\hat{a}^\dagger\hat{a}\rangle = \gamma_n$, so individual trajectories "deconstruct" in a decoherence time $(\gamma n)^{-1}$, as shown in Fig. 15. The n-photon Wigner function, the Laguerre polynomial $\mathcal{L}_n$ jumps to $\mathcal{L}_{n-1}$ at random times, with probability γ_n. The average over many trajectories reproduces the density matrix solution of eq. (169).

So far, we have discussed the quantum jumps in a single-component field state. We now turn our attention to superpositions. In Fig. 16 we illustrate the time-evolution of a single ensemble member of a Schrödinger cat state of the form $(|\alpha\rangle+|-\alpha\rangle)/N_+(\alpha)$, where $N_+(\alpha)$ is the normalization, and $|\alpha\rangle$ and $|-\alpha\rangle$ are two coherent states, as it undergoes two quantum jumps. During the time interval

Figure 16: A "jumping cat" which was initially comprised of the coherent states $|\alpha\rangle$ and $|-\alpha\rangle$ with $\alpha = 2$. We show the Wigner functions before and after the first jump (at $\kappa t = 0.668$) in (a) and (b). In (c) and (d) we show the Wigner functions before and after the second jump (at $\kappa t = 1.884$).

when there are no jumps, the Schrödinger cat shrinks as $\alpha(t) = \alpha(0)\, e^{-\gamma t/2}$ when the evolution (eq.(180)) is considered. This no-jump process has taken place from the initial state up to Fig. 16(a). When there is a jump, then according to eq.(179), we find that the cat jumps to a different kind of cat, of the form $(|\alpha(t)\rangle - |-\alpha(t)\rangle)/N_-(\alpha(t))$. This jump is seen as we go from Fig. 16(a) to Fig. 16(b). This jump from an even to an odd cat is particularly visible in the Wigner functions because the interference fringes change sign. Subsequently the cat shrinks again as we evolve under the no-jump evolution again. This takes us to Fig. 16(c) as the components shrink towards the origin. Finally we portray the effect of a second jump, where once again the interference fringes change sign. Decoherence results from the ensemble average over these uncontrollable phase jumps.

5 Quantum Jumps

5.1 Intrinsic or Extrinsic Jumps

So far, we have discussed the evolution of *open* systems, that is of microsystems in contact with Markovian reservoirs such as the bath of vacuum field modes responsible for spontaneous emission. The quantum jump concept within an open system context has to do with the gain in information about the microsystem which is accessible from the record available in the dissipative environment. Such jump processes do *not* require an extension or modification of conventional quantum mechanics, and we will refer to these as "extrinsic" jumps. A very different jump mechanism has been studied by a number of authors [47] and especially by Ghirardi, Rimini and Weber [48]. In these approaches the Schrödinger equation is modified in such a way that quantum coherences are automatically destroyed in a *closed* system by an *intrinsic* stochastic jump mechanism. This should be distinguished from the extrinsic mechanisms we are concerned with in the bulk of these lectures.

To see how an intrinsic jump mechanism works, we need a concrete realisation which we can apply to a specific time evolution. Milburn has proposed just such a realisation [49], in which standard quantum mechanics is modified in a simple way to generate intrinsic decoherence. He assumes that on sufficiently short time steps, the system does not evolve continuously under normal unitary evolution, but rather in a *stochastic* sequence of identical unitary transformations. This assumption leads to a modification of the Schrödinger equation which contains a term responsible for the decay of quantum coherence in the energy eigenstate basis, without the intervention of a reservoir and therefore without the usual energy dissipation associated with normal decay [50]. The decay is entirely of phase-dependence only, akin to the dephasing decay of coherences produced by impact-theory collisions or by fluctuations in the phase of a laser in laser spectroscopy, but here of intrinsic origin.

It is interesting to apply Milburn's model of intrinsic decoherence to a problem of dynamical evolution: that is, the interaction of two subsystems and the coherences which establish themselves as a consequence of their interaction. We have considered [50] the interaction between a single two-level atom and a quantized cavity mode and shown how the intrinsic decoherence affects the long–time coherence characteristics of the entangled atom–field system. In particular we have shown how the revivals (a signature of long–time coherence) are removed by this intrinsic decoherence.

5.2 Observation of Quantum Jumps

We now return to *conventional* quantum mechanics but of *open* systems: systems interacting with a Markovian environment, in which jumps are the result of irreversible emissions into the external bath which can be detected to give a record of the open system dynamics. In a real sense, the jumps in an open system are jumps in our knowledge of the state of the system. Individual, repeatable, jumps were in the past obscured by the statistical averaging necessary when observing an ensemble of very many identical systems. But developments in experimental techniques, especially in quantum optics have enabled us to observe the dynamics of single quantum systems: fields can be trapped in high Q cavities and manipulated by interaction with individual atoms, and single electrons and ions can be trapped and shielded for very long periods of time. In 1975, Dehmelt [51] suggested the use of trapped three-level ions to make visible quantum jumps in a configuration he termed an atomic amplifier. The configuration is shown in Fig. 17. The $1-0$ transition is strongly allowed so that of order 10^7 photons per second are emitted when that transition is strongly-driven. The state 2 is chosen to be metastable: lifetimes of seconds have been used. The rare (because of the transition being weak) excitation events to state 2 will terminate the strong fluorescence and lead to a period of "darkness" which persists until the ion decays back to the ground state 0. The probability of remaining in the "shelving" state 2 introduces an element of randomness in the duration of the dark periods. The *lack* of fluorescence constitutes a measurement of the $0-2$ transition (a *null* result of a measurement is still a measurement and leads to a gain in information about the system [52]). The further study of this shelving process was stimulated by a paper by Cook and Kimble [53] who described how the three-level ion shelving scheme leads to a random telegraph fluorescence signal, where the observed fluorescence turns on and off abruptly as the ion is shelved and decays at random. This triggered a substantial experimental effort and resulted in a number of observations of the telegraphic quantum jumps in three-level ion fluorescence [54]. It is worth noting that jumps in the excitation levels of a single electron trapped in a Penning trap were already observed in 1977 [55] although this does not involve fluorescence detection, of course. Shelving is an essential building block of trapped ion frequency standards [56].

It is worth studying the dynamics of a three-level ion in this shelving situ-

Figure 17: Dehmelt's atomic amplifier, in which a three-level trapped ion is excited by two incident light fields; level 1 is readily excited and is a normal state which strongly fluoresces back to the ground state 0, whereas state 2 is metastable. Excitation to state 2 will interrupt the $1-0$ fluorescence for a period until the ion decays back to 0 and enables the strong $0-2$ resonance fluorescence to recommence. The lack of strong fluorescence during the temporary shelving induced by a single photon absorption to state 2 is the "amplification".

Figure 18: Time-evolution of the population in the strongly-fluorescing level 1 of the three-level ion shown in Fig. 14. The lifetimes γ_1^{-1} and γ_2^{-1} are marked on the time axis. What is crucial here is the "hump" $\Delta\rho_{11}$: this is a signature of the telegraphic nature of the fluorescence.

ation to see how the bright and dark periods are determined by the excitation dynamics. Provided the $0-1$ and $0-2$ Rabi frequencies are small compared with the decay rates, we find for the population in the strongly-fluorescing level 1 as a function of time something like the behaviour shown in Fig. 18. We choose for this figure the values $\gamma_1 \gg \gamma_2$, reflecting the metastability of level 2. For times short compared with the metastable lifetime γ_2^{-1}, then of course the atomic dynamics is hardly aware of level 2 and evolves as a $0-1$ *two-level* system. After a time γ_2^{-1}, the metastable state has an effect and the (ensemble-averaged) population in level 1 reduces to the appropriate *three-level* equilibrium values. The "hump" $\Delta\rho_{11}$ shown in Fig. 18 is actually a signature of the telegraphic fluorescence. To show this, consider a few sequences of bright and dark periods in the telegraph signal as shown in Fig. 19. The total rate of emission R is proportional to the bright rate times the fraction of the evolution made up of bright periods:

$$R = \left(\frac{T_B}{T_B + T_D} \right) \bar{\rho}_{11} \tag{185}$$

but this has to be equal to the true average,

$$R = \rho_{11}(\infty) \, , \tag{186}$$

Figure 19: A few periods of bright and dark sequences in the fluorescence intensity I from a three-level system. The bright periods last on average T_B, and the dark periods T_D.

so that

$$\frac{T_D}{T_B} = \frac{\bar{\rho}_{11} - \rho_{11}(\infty)}{\rho_{11}(\infty)} = \frac{\Delta\rho_{11}}{\rho_{11}(\infty)}\,, \tag{187}$$

and the ratio of the period of bright to dark intervals is governed, as we claimed, by the "hump" $\Delta\rho_{11}$.

So far, we have concentrated on situations where the Rabi frequencies are small (or for incoherent excitation). What happens for *coherent* resonant excitation with larger Rabi frequencies? The answer to this naive question is *nothing*: there are essentially *no* quantum jumps at least at any significant level for coherently-driven resonantly excited three-level systems! But this is because of the idea of resonance is tricky: the strong $0-1$ Rabi frequency dresses the atom and AC-Stark splits the transition, forcing the system substantially out of resonance. If this is recognized and the probe laser driving the $0-2$ transition is detuned from the bare resonance until it matches the dressed atom resonance, then the jumps and telegraphic fluorescence return. As far as we know, the dependence of the telegraph fluorescence on detuning for coherently excited transitions has yet to be investigated experimentally.

Let us return to the idea of a null measurement. We imagine that we observe the fluorescence from a driven three-level ion over a time scale which is long compared with the strongly fluorescing state lifetime γ_1^{-1} but very short compared with the shelf state lifetime γ_2^{-1}, so that $\gamma_1^{-1} \ll \Delta t \ll \gamma_2^{-1}$. Pegg and Knight [57] have shown that the average period of brightness and darkness in

the telegraphic fluorescence can be obtained from considerations of null detection. During such an interval Δt, the population in the shelf state, $P_2(t)$ hardly has time to evolve, but population can be rapidly cycled from the ground state $|0\rangle$ to the strongly-fluorescing state $|1\rangle$ and back. Detection of a photon at the beginning of a Δt interval implies a survival in the 0 – 1 sector for the whole interval and a bright period, whereas a *null* detection is sufficient for us to be confident that the atom is shelved for the whole Δt interval and a dark period ensues.

If we take our origin of time to be after an interval Δt in which we see a photon, then $P_2(0) = 0$. We can introduce the "life expectancy" T_B as the time the atom spends in the 0 – 1 sector *continuously*. If the atom is still in this sector at a time t_1 (known from an observation of another fluorescence photon just prior to t_1), then the life expectancy will be also T_B. So we can partition the outcomes into the case where at t_1 it has survived in the 0 – 1 sector with probability $P_{10}(t_1)$ and the case where the ion did not survive the whole interval t_1 continuously in the 0 – 1 sector [57]

$$T_B = P_{10}(t_1)\,(t_1 + T_B) + (1 - P_{10}(t_1))ft_1\,, \tag{188}$$

where f is a fraction (< 1). Then for small t_1,

$$T_B = \frac{t_1 P_{10}(t_1)}{1 - P_{10}(t_1)} = \frac{t_1}{1 - P_{10}(t_1)} - t_1 \tag{189}$$

and if t_1 is small so we may neglect the possibility of a *return* from state $|2\rangle$ back in to the 0 – 1 sector, $(1 - P_{10}(t_1)) \approx P_2(t_1)$, so that

$$T_B^{-1} = \left.\frac{dP_2}{dt}\right|_{t=0} \quad \text{given} \quad P_2(0) = 0\,. \tag{190}$$

This is finite, so we know that the fluorescence *will* terminate. To obtain a value for T_B, we merely need to know the evolution equation (not its solution) for the population in state $|2\rangle$: this would be the Bloch equation for coherent excitation, or the Einstein rate equation for incoherent excitation.

The calculation of the mean period of darkness proceeds along similar lines: if *no* photons are detected in an interval Δt just before $t = 0$, we find

$$T_D^{-1} = -\left.\frac{dP_2}{dt}\right|_{t=0} \quad \text{given} \quad P_2(0) = 1\,. \tag{191}$$

Estimates of T_B and T_D are readily obtainable if the 0 – 1 transition is saturated. If $P_2(0)$ is found to be zero, then $P_1 = 1/2 = P_0$, then

$$\left.\frac{dP_2}{dt}\right|_{t=0} \approx \left(\begin{array}{c}\text{stimulated rate}\\ \text{out of 0 to 2}\end{array}\right) \times P_0(0)$$

and $T_B^{-1} = R/2$, where R is this stimulated rate. The average dark period is found to be $T_D = 1/R$ by similar arguments [57]. This shows that the random telegraph signal for saturated transitions has bright periods lasting two times longer on average than the dark periods. Pegg and Knight [57] have estimated the characteristic time to be sure that a quantum jump has occurred.

Let us now return to the Monte-Carlo simulation of quantum jumps. For purely spontaneous emission from a two-level atom, the relevant density operator master equation is

$$\begin{aligned} \dot{\rho_S} &= -\frac{i}{\hbar}[H, \rho_S] - \frac{\gamma}{2}(\hat{\sigma}_+\hat{\sigma}_-\rho_S + \rho_S\hat{\sigma}_+\hat{\sigma}_-) \\ &\quad + \gamma\hat{\sigma}_-\rho_S\hat{\sigma}_+ \,. \end{aligned} \tag{192}$$

The operators $\hat{\sigma}_\pm$ are the usual Pauli raising and lowering operators (see section 8 for more details), H is the two–level system Hamiltonian and γ the spontaneous emission rate. To propagate the conditioned state vector from time t to $(t + \Delta t)$ we need to calculate the current probability of emission, given by

$$\Delta p = \gamma\Delta t\langle\Psi(t)|\hat{\sigma}_+\hat{\sigma}_-|\Psi(t)\rangle \,. \tag{193}$$

Then the jump probability Δp is compared with a computer-generated random number r. If $r < \Delta p$, then as before, we re-set the state according to the lowering operator

$$|\Psi\rangle \longrightarrow N^{-1}\hat{\sigma}_-|\Psi\rangle \tag{194}$$

where N^{-1} is a normalization factor. If, on the other hand $\Delta p < r$, then we take the no-jump possibility and propagate $|\Psi\rangle$ under the influence of the non-Hermitian effective Hamiltonian $H_{\rm eff} = H - i\hbar\frac{\gamma}{2}\hat{\sigma}_+\hat{\sigma}_-$, where H is the unperturbed atomic Hamiltonian, so that

$$|\Psi\rangle \longrightarrow N^{-1}(1 - H_{\rm eff}\Delta t/\hbar)|\Psi\rangle \,. \tag{195}$$

A single trajectory evolves in a smooth evolution under $H_{\rm eff}$, interrupted by the jumps. Bouwmeester and colleagues [58] have discussed the physical interpretation of the no-jump evolution and connected this to the decay behaviour in Jaynes "neoclassical theory" [59]. When many trajectories are averaged, the traditional exponential decay law is recovered.

Resonance fluorescence can be described by a modest extension of the above: all one needs to do is to supplement H by a term describing the coupling of an external laser driving field to the atomic dipole, so that

$$H = \Delta\hat{\sigma}_+\hat{\sigma}_- + (g\hat{\sigma}_+ + g^*\hat{\sigma}_-) \tag{196}$$

where the detuning between the atomic frequency ω and the laser frequency Ω is $\Delta = \omega - \Omega$, and the coupling constant g is given by one half of the Rabi frequency $(-\wp\mathcal{E}_\Omega/\hbar)$ where $\wp$ is the atomic dipole moment and $\mathcal{E}_\Omega$ is the amplitude of the laser driving field. Given that the laser field can re-excite the atom,

Figure 20: Three-level scheme to illustrate quantum telegraph signal in fluorescence from a three-level system. The $0-1$ transition is strongly allowed and resonantly excited; state 1 decays at a rate γ_1. State 2 is metastable, with a long lifetime γ_2^{-1}, so that $\gamma_2 \ll \gamma_1$, and is excited by a field which may be detuned by an amount Δ_2 from the bare $0-2$ resonance.

a single trajectory now evolves with many quantum jumps, and an ensemble average over many trajectories reproduces the behaviour predicted from the Bloch equations. This procedure can be generalized to multilevel atoms, and in particular to the three-level lambda system traditionally used to generate the quantum telegraphic "shelving" fluorescence so characteristic of quantum jumps. In Fig. 20 we indicate the level scheme under consideration. The $0-1$ transition is strongly driven, whereas state 2 is assumed to be a metastable state weakly probed by a much less intense laser field; we allow a small detuning of the probe laser from the $0-2$ transition. The strong driving of the $0-1$ transition Stark shifts the position of state 0, and hence the $0-2$ transition is shifted from its bare transition to a dressed position; the detuning can be adjusted to compensate for this. If this detuning is ignored and bare resonance is maintained, essentially *no* telegraphic signal is generated as we discussed earlier, whereas if the detuning appropriate to the Stark-shifted resonance is maintained, the telegraphic excitation can proceed [60]. In Fig. 21 we show the result of a Monte-Carlo wavefunction simulation of these quantum jumps. We see periods where the population resides in state 1 (and can fluoresce) interspersed with periods where the atom is "shelved" in state 2. The rival effects of coherent excitation and of jumps is quite interesting here and will be discussed elsewhere [61]. We have also used this method to describe the so called "Quantum Zeno

Figure 21: Results of a simulation of the population ρ_{11} in the strongly-fluorescing state 1 in the three-level shelving scheme. For this simulation we set $\Omega_1/\gamma_1 = 2.5$, $\Omega_2/\gamma_1 = 0.1$, $\Delta/\gamma_1 = 2.5$, $\gamma_2/\gamma_1 = 0.005$.

effect" of freezing time evolution through frequent, repeated observations [62].

6 Quantum State Diffusion

The second simulation method we consider is quantum state diffusion in which the evolution of $|\Psi(t)\rangle$, representing one member of the ensemble, is determined by a non-linear stochastic differential equation [63, 64]. We write the equation (for the specific case of one-photon damping of a field state) in the Itô form involving drift and diffusion processes so that

$$\begin{aligned} |\Psi(t+\delta t)\rangle &= (1 - i\delta t H)\,|\Psi(t)\rangle + \kappa\left[\langle\hat{a}^\dagger\rangle\hat{a} - \tfrac{1}{2}\hat{a}^\dagger\hat{a} - \tfrac{1}{2}\langle\hat{a}^\dagger\rangle\langle\hat{a}\rangle\right]|\Psi(t)\rangle\,\delta t \\ &\quad + \sqrt{\kappa}\left[\hat{a} - \langle\hat{a}\rangle\right]|\Psi(t)\rangle\,\mathrm{d}\xi_t \end{aligned} \tag{197}$$

where $\mathrm{d}\xi_t$ is a random complex Wiener variable which perturbs the system. It varies randomly between each time step and each sample run so that when averaged:

$$\overline{\mathrm{d}\xi_t} = 0 \quad , \quad \overline{\mathrm{d}\xi_t \mathrm{d}\xi_{t'}} = 0 \quad , \quad \overline{\mathrm{d}\xi_t^* \mathrm{d}\xi_{t'}} = \delta_{t,t'}\,\delta t\,. \tag{198}$$

In consequence the time evolution is not smooth on a very small scale because of the discretised fluctuations of the state vector in its Hilbert space. This distinguishes the quantum state diffusion calculations from the state vector Monte-Carlo approach in a characteristic way; in the latter case the state

vector (and hence the observables) jump only at certain places rather than at every time point. This manifestation of the constant jiggling of the state vector is clearly seen in the single trajectory examples of Fig. 22 (solid and dotted curves). However, as in the state vector Monte-Carlo the results for an ensemble average smooth out as we increase the number of samples.

It is interesting to note that if it happens that $|\Psi(t)\rangle$ is an eigenstate of the Lindblad operator $\hat{a}$, then the random fluctuations do not contribute to the system evolution in (197). This results in a vanishing of the random perturbations as can be seen in Fig. 22 as equilibrium is established. That $|\Psi(t)\rangle$ is an eigenstate of $\hat{a}$ is not a sufficient condition for the steady state; an inspection of eq. (197) shows that we also require $|\Psi(t)\rangle$ to be an eigenstate of $H - \frac{1}{2}i\hat{a}^\dagger\hat{a}$ as is found in the state vector Monte-Carlo case.

The stochastic equation (197) amounts to a Langevin equation for the state vector (rather than the usual case of observables). As in the case of state vector Monte-Carlo simulations we can recover the master equation (170) when we average over the ensemble. Equation (197), constructed by Gisin and Percival, has recently been interpreted as the state vector evolution in a balanced heterodyne detection scheme [65]. A related equation is found for the case of balanced homodyne detection by Carmichael [5]. In both cases a quantum jump theory is developed for the measurement process in the presence of a strong classical local oscillator. This quantum jump theory, unlike the single mode case presented above, contains two jump operators, i.e. one for each of the detectors. Using the fact that the local oscillator is strong and creates many jumps in the detector, the number of jumps in a short time interval can be determined by a stochastic function $\mathrm{d}\xi$ as found in eq. (197) above. Imagine, for definiteness, the heterodyne situation shown in Fig. 23. The two heterodyne output modes $\hat{c}_1, \hat{c}_2$ are superpositions of input modes $\hat{a}$ (describing the quantum system of interest) and $\hat{b}$ (describing the local oscillator, which we imagine to be in a coherent state $|\beta\rangle$ of amplitude $|\beta| \gg 1$). Then for a 50% transmitting beam-splitter [8],

$$\begin{aligned} \hat{c}_1 &= \frac{1}{\sqrt{2}}\,(\hat{a} + \hat{b})\,, \\ \hat{c}_2 &= \frac{1}{\sqrt{2}}\,(\hat{a} - \hat{b})\,. \end{aligned} \tag{199}$$

The two detectors count photons in the output modes, so we introduce jump operators $\hat{J}_1$ and $\hat{J}_2$ for these detectors

$$\begin{aligned} \hat{J}_1 &= \gamma^{1/2}\hat{c}_1\,, \\ \hat{J}_2 &= \gamma^{1/2}\hat{c}_2\,. \end{aligned} \tag{200}$$

Within a short time Δt we will count many jumps, because of the large amplitude of the local oscillator field β; the total number of counted jumps in Δt will fluctuate in number to lead to a stochastic evolution. Note that

$$\hat{c}_1^\dagger\hat{c}_1 = \frac{1}{2}\,(\hat{a}^\dagger\hat{a} + \hat{b}^\dagger\hat{b} + \hat{a}^\dagger\hat{b} + \hat{b}^\dagger\hat{a}) \tag{201}$$

Figure 22: Localization of a Schrödinger "cat" state which is initially comprised of the coherent states $|\alpha\rangle$ and $|-\alpha\rangle$ with $\alpha = 2$. We show $\langle\hat{X}\rangle$ (solid curve—left-hand scale) and ΔX (dotted curve—right-hand scale). The localization is seen in the development of the non-zero value of $\langle\hat{X}\rangle$ and in the rapid reduction of the uncertainty. The dashed curve shows ΔX for the quantum jump trajectory of Fig. 16. The value of $\langle\hat{X}\rangle$ is zero in this case because there is no localization.

Figure 23: Heterodyne measurement of cavity field $\hat{a}$ by mixing at a beam-splitter a local oscillator field $\hat{b}$ (assumed to be in an intense coherent state $|\beta\rangle$, $|\beta| \gg 1$) followed by detection of the two output fields described by the operators $\hat{c}_1, \hat{c}_2$.

and the local oscillator is in the coherent state $|\beta e^{i\phi}\rangle$. Then

$$\langle \hat{c}_1^\dagger \hat{c}_1 \rangle = \frac{1}{2} \langle \hat{a}^\dagger \hat{a} + \beta^2 + \hat{a}^\dagger \beta e^{i\phi} + \hat{a} \beta e^{-i\phi} \rangle \tag{202}$$

and similarly

$$\langle \hat{c}_2^\dagger \hat{c}_2 \rangle = \frac{1}{2} \langle \hat{a}^\dagger \hat{a} + \beta^2 - \hat{a}^\dagger \beta e^{i\phi} - \hat{a} \beta e^{-i\phi} \rangle \, . \tag{203}$$

In balanced heterodyne measurement, the difference in counts of the two detectors is measured so that the terms $\langle \hat{a}^\dagger \hat{a} \rangle$ and β^2 cancel, and we see that the difference is given by the mean value of the quadrature operator $\hat{x}_\phi = (1/2) \, (\hat{a}^\dagger e^{i\phi} + \hat{a} e^{-i\phi})$:

$$\begin{aligned} \langle \hat{c}_1^\dagger \hat{c}_1 \rangle - \langle \hat{c}_2^\dagger \hat{c}_2 \rangle &= \beta \langle \hat{a}^\dagger e^{i\phi} + \hat{a} e^{-i\phi} \rangle \\ &\equiv 2\beta \langle \hat{x}_\phi \rangle \, . \end{aligned} \tag{204}$$

To simulate the heterodyne measurement, we need to define the effective non-Hermitian evolution $H_{\rm eff}$ which governs the no-jump events. We set

$$\begin{aligned} H_{\rm eff} &= -\frac{i\hbar}{2} \, (\hat{J}_1^\dagger \hat{J}_1 + \hat{J}_2^\dagger \hat{J}_2) \\ &\approx -i\hbar \frac{\gamma}{2} \, (\hat{a}^\dagger \hat{a} + \beta^2) \end{aligned} \tag{205}$$

where the second form follows if we assume the local oscillator to be in an intense coherent state $|\beta e^{i\phi}\rangle$ and neglect its quantum nature. Then the no-jump evolution is given by

$$\exp \left(-i H_{\rm eff} \Delta t / \hbar \right) \approx 1 - \frac{\gamma}{2} \, (\hat{a}^\dagger \hat{a} + \beta^2) \Delta t \, . \tag{206}$$

The jump operators we take in the same approximation as

$$\begin{aligned} \hat{J}_1 &= (\frac{\gamma}{2})^{1/2} \, (\hat{a} + \beta e^{i\phi}) \, , \\ \hat{J}_2 &= (\frac{\gamma}{2})^{1/2} \, (\hat{a} - \beta e^{i\phi}) \end{aligned} \tag{207}$$

so that the probabilities of jumps per unit time are given by

$$\begin{aligned} \langle \hat{J}_1^\dagger \hat{J}_1 \rangle &\sim \frac{\gamma}{2} \, \beta^2 \, (1 + (2/\beta) \langle \hat{x}_\phi \rangle) \approx \gamma \beta^2 / 2 \, , \\ \langle \hat{J}_2^\dagger \hat{J}_2 \rangle &\sim \frac{\gamma}{2} \, \beta^2 \, (1 - (2/\beta) \langle \hat{x}_\phi \rangle) \approx \gamma \beta^2 / 2 \, . \end{aligned} \tag{208}$$

We choose the interval time Δt to be large enough to contain many detected counts, but small compared with the system evolution time. Then the total number of detected jumps is $\langle \hat{J}_i^\dagger \hat{J}_i \rangle \Delta t$ (where $i = 1, 2$) on average, though it fluctuates.

If we divide up the interval Δt into n segments of length δt, then the probability of m counts is

$$P(m) = \frac{n!}{(n-m)!\,m!}(P\delta t)^m(1-P\delta t)^{n-m}\,. \tag{209}$$

But since $P\Delta t \gg 1$, we can approximate this by the Gaussian form

$$P(m) = \left((2\pi)^{1/2}\sigma\right)^{-1} \exp\left[-(m-P\Delta t)^2/2\sigma^2\right] \tag{210}$$

where

$$\sigma^2 = P\Delta t(1-P\delta t) \approx P\Delta t\,. \tag{211}$$

In other words,

$$P(m) = \frac{1}{(2\pi\langle\hat{J}^\dagger\hat{J}\rangle\Delta t)^{1/2}} \exp\left[-\frac{1}{2}\frac{(m-\langle\hat{J}^\dagger\hat{J}\rangle\Delta t)^2}{\langle\hat{J}^\dagger\hat{J}\rangle\Delta t}\right] \tag{212}$$

where

$$m(t) = \hat{J}^\dagger\langle\hat{J}\rangle\Delta t + (\langle\hat{J}^\dagger\hat{J}\rangle)^{1/2}\Delta W \tag{213}$$

and the Wiener noise term is such that

$$\langle\Delta W^2\rangle = \Delta t\,. \tag{214}$$

To use the jump method, we need to evaluate powers of the jump operators: if there are m detected counts in Δt, then we will need

$$\begin{aligned}(\hat{J}_1)^{m_1} &= \left[\beta(\frac{\gamma}{2})^{1/2}\,(1+\frac{\hat{a}}{\beta}\,e^{-i\phi})\right]^{m_1} \\ &\propto \left(1+\frac{m_1}{\beta}\hat{a}e^{-i\phi}\right) \quad , \beta \gg 1\,.\end{aligned} \tag{215}$$

Similarly

$$(\hat{J}_2)^{m_2} \propto \left(1-\frac{m_2}{\beta}\hat{a}\,e^{-i\phi}\right)\,, \tag{216}$$

where

$$m_i = \langle\hat{J}_i^\dagger\hat{J}_i\rangle\Delta t + (\langle\hat{J}_i^\dagger\hat{J}_i\rangle)^{1/2}\,\Delta W_i \quad (i=1,2)\,. \tag{217}$$

The un-normalized evolution over Δt is given by

$$|\Psi\rangle \longrightarrow \exp\left(-iH_{\rm eff}\Delta t/\hbar\right)(\hat{J}_1)^{m_1}(\hat{J}_2)^{m_2}|\Psi\rangle\,, \tag{218}$$

where the operator ordering is not important with the approximations used. Using the results above, we find

$$|\Psi\rangle \longrightarrow \left[1-iH_{\rm eff}\Delta t/\hbar + \beta^{-1}\hat{a}e^{-i\phi}(m_1-m_2)\right]|\Psi\rangle \tag{219}$$

so that

$$|\Psi\rangle \longrightarrow \left[1 - iH_{\rm eff}\Delta t/\hbar + e^{-i\phi}\frac{\hat{a}}{\beta}(2\gamma\,\beta\,\langle\hat{x}_\phi\rangle\Delta t + \beta\,(\frac{\gamma}{2})^{1/2}(\Delta W_1 - \Delta W_2))\right]|\Psi\rangle\,. \tag{220}$$

We will add together the two Wiener increments as $\Delta W = (\Delta W_1 + \Delta W_2)/\sqrt{2}$, and from now on write all increments in terms of differentials, e.g. dW. Now the local oscillator and the quantum system have different frequencies, so the time dependent phase $\phi(t)$ can be incorporated into the definition of the Wiener increment, as $e^{-i\phi(t)}\,dW \to dW_c$. We find, after all this, the stochastic evolution equation

$$|d\tilde{\Psi}\rangle \sim \left[-\frac{\gamma}{2}(\hat{a}^\dagger\hat{a} + \beta^2)dt + \gamma\hat{a}\langle\hat{a}^\dagger\rangle dt + \sqrt{\gamma}\,\hat{a}\,dW_c\right]|\Psi\rangle \tag{221}$$

which is one form of the nonlinear stochastic evolution equation characteristic of the Quantum State Diffusion model [63] and where $|\tilde{\Psi}\rangle$ is the state $|\Psi\rangle$ before normalization.

To obtain the equation of motion for the normalized state vector one has to be careful about differentiation because of the normalization of the noise term (Eq. (198)). The Itô calculus may be used under which, for example,

$$\mathrm{d}(\langle\tilde{\Psi}(t)|\tilde{\Psi}(t)\rangle) = \langle\tilde{\Psi}(t)|\mathrm{d}\tilde{\Psi}\rangle + \langle\mathrm{d}\tilde{\Psi}|\tilde{\Psi}(t)\rangle + \langle\mathrm{d}\tilde{\Psi}|\mathrm{d}\tilde{\Psi}\rangle\,. \tag{222}$$

Furthermore, to obtain a connection with the Gisin-Percival equation (197) it is necessary in the spirit of Gisin and Percival, to include a phase factor as well as renormalizing the state vector so that

$$|\Psi(t)\rangle = \frac{e^{i\zeta(t)}|\tilde{\Psi}(t)\rangle}{\sqrt{\langle\tilde{\Psi}(t)|\tilde{\Psi}(t)\rangle}}\,. \tag{223}$$

The phase factor is stochastic because

$$i\mathrm{d}\zeta = \frac{\langle\tilde{\Psi}(t)|\hat{a}^\dagger|\tilde{\Psi}(t)\rangle\mathrm{d}\xi^* - \langle\tilde{\Psi}(t)|\hat{a}|\tilde{\Psi}(t)\rangle\mathrm{d}\xi}{2\langle\tilde{\Psi}(t)|\tilde{\Psi}(t)\rangle} \tag{224}$$

resulting in the equation for the normalized $|\Psi(t)\rangle$:

$$\begin{aligned}
|\mathrm{d}\Psi\rangle \;=\;& \kappa\left[-\tfrac{1}{2}\hat{a}^\dagger\hat{a} + \hat{a}\langle\Psi(t)|\hat{a}^\dagger|\Psi(t)\rangle + \tfrac{1}{2}\langle\Psi(t)|\hat{a}^\dagger\hat{a}|\Psi(t)\rangle\right.\\
&\left. - \langle\Psi(t)|\hat{a}^\dagger|\Psi(t)\rangle\langle\Psi(t)|\hat{a}|\Psi(t)\rangle\right]|\Psi(t)\rangle\mathrm{d}t\\
&+ \tfrac{1}{2}\kappa\left[-\langle\Psi(t)|\hat{a}^\dagger\hat{a}|\Psi(t)\rangle + \langle\Psi(t)|\hat{a}^\dagger|\Psi(t)\rangle\langle\Psi(t)|\hat{a}|\Psi(t)\rangle\right]|\Psi(t)\rangle\mathrm{d}\xi^*\mathrm{d}\xi\\
&+ \sqrt{\kappa}\left[\hat{a} - \langle\Psi(t)|\hat{a}|\Psi(t)\rangle\right]|\Psi(t)\rangle\mathrm{d}\xi\,.
\end{aligned} \tag{225}$$

This equation yields the Gisin-Percival equation (197) if $\mathrm{d}\xi^*\mathrm{d}\xi \longrightarrow \mathrm{d}t$. The only difference between these equations is that the state vector in eq. (197) is only

normalized for the ensemble average whilst in eq. (225) it is always normalized. In practice this seems to result in no noticeable differences because whilst our computer program integrates eq. (197) it renormalizes the state vector at every time step.

We should emphasize that the non-linear equations we consider here in no way violate the principles of quantum mechanics. Each kind of simulation is non-linear because it is conditional on a specific unravelling of the master equation (170) and when we ensemble average over a large number of state vectors we always recover the master equation (170) with the appropriate reservoir operators [5, 45, 63, 66].

In Fig. 24 we demonstrate the process by which the state localises in quantum state diffusion from an initial superposition by plotting the Wigner function. Interference fringes can be seen in the initial state, Fig. 24(a), which consists of a Schrödinger "cat" coherent superposition of two coherent states $|\alpha\rangle$ and $|-\alpha\rangle$ (with $\alpha = 2$ in this case), with the two components representing the live "cat" and the dead "cat". If we now examine the time sequence in Figs.24(a-d) we observe that one of the components of the "cat" diminishes as the other component grows. This is accompanied by a rapid loss of the fringes. The Wigner function clearly shows localization to one of the coherent state components of the original "cat", the choice of component being determined randomly according to the stochastic input. In Fig. 22 we show the values of the quadrature $\langle \hat{X} \rangle = \langle \Psi(t) | (\hat{a} + \hat{a}^\dagger) | \Psi(t) \rangle / 2$ and uncertainty $\Delta X = (\langle \hat{X}^2 \rangle - \langle \hat{X} \rangle^2)^{1/2}$ as a function of time and including the times at which the Wigner functions of Fig. 24 are appropriate. The localization manifests itself in $\langle \hat{X} \rangle$ through the rapid development of a non-zero value of the displacement which takes place as one of the component coherent states is chosen. Subsequently, the value of $\langle \hat{X} \rangle$ decays as the coherent state itself approaches the ground state. The localization is seen in ΔX as a rapid reduction (at essentially the decoherence rate $\gamma |\alpha|^2$) to a value of one half, the uncertainty value for a coherent state. The value of one half is maintained as the coherent state dissipates to the origin. The picture would be quite different if we were to consider the density matrix approach. In that case the fringes in the Wigner function would also rapidly disappear, but we would be left with both of the components reflecting a statistical mixture of outcomes [67].

We have so far presented the heterodyne experiment with a simple choice of two components (outcomes) of a Schrödinger "cat". Any state of the oscillator can be represented as a superposition of coherent states, and the quantum state diffusion will describe localization to a single coherent state component. We next consider a complex superposition of coherent states: a Fock state. As mentioned earlier a continuous superposition of coherent states with any radius r can form a Fock state provided the correct phase factors $e^{-in\theta}$ are present. However, when localization takes place a coherent state is selected from that circle for which each component coherent state has nearly the same energy as the original Fock state. The process is illustrated in Fig. 25. The initial state in (a) contains

Figure 24: Wigner functions from the quantum state diffusion of a single sample. We see $\gamma t = 0, 0.05, 0.2$ and 0.8 in (a-d). Localization is seen as the increasing dominance of one component of the "cat".

nine quanta and its Wigner function, formed from a Laguerre polynomial, is made up of an outer rim with inner concentric fringes. As time progresses, (b,c), we observe that localization starts with the preferential orientation of the rim and fringes in one direction. This chosen direction is different for each realization. As the outer rim localizes, the inner fringes wash out with the vanishing of quantum interference between coherent state components. In (d) we see that the fringes have almost disappeared and the remaining localized state approaches a coherent state. In this case, the localization rate is much less than the decoherence rate: in order to localize, sufficient decay time has to elapse to generate a range of photon numbers to support the full Poisson width of a coherent state component. During the subsequent time evolution the Wigner function becomes quite rounded and moves in towards the phase-space origin. We have also investigated the localization from initially squeezed states, and again we see localization into components of eq. (153) (and under some conditions, the formation of *Schrödinger "cats"*).

7 Comparison of Ensemble Averaged Results

We have seen in the previous two sections how the state vector Monte-Carlo method and quantum state diffusion method of simulation lead to very different behaviour for individual realizations and reflect the gain in information from specific conditionings, whilst for an average over large samples they realise the results of the master equation (170). In the case where we are only interested in ensemble averages, we can treat each simulation merely as a computational algorithm en route to an ensemble behaviour and ignore the subtleties of how each simulation reflects a specific conditioning. However, in all practical cases the number of samples must be finite. Then given that we may have a choice of the two methods for performing the simulation the question arises as to which to use: when ensemble averaged, both methods seem to give results with about the same accuracy. In order to check this we have calculated the mean fluctuations between simulated, and sample averaged, observables and the computed observables from direct integration of the master equation (170) in a similar fashion to the two photon processes examined in [66]. Here we consider one-photon decay and the fluctuations are averaged over the time evolution and are shown in Fig. 26 for the observable $\langle \hat{n} \rangle$ where the symbols $\times$ indicate the fluctuations with the state vector Monte-Carlo approach and the symbols $+$ show fluctuations in quantum state diffusion. The fluctuations decrease in size with sample number roughly as expected from the central limit theorem. However, these results also depend on the integration step size δt and can only be taken as representative. For example, if the step size is reduced, then greater accuracy may be achieved with larger numbers of samples.

Figure 25: Localization of a Fock state $|n\rangle$ with $n = 9$. These results are for a single sample undergoing quantum state diffusion. The Wigner functions are shown for $\kappa t = 0, 0.1, 0.5$ and 1.0 in (a-d).

Figure 26: Error in simulation as a function of sample size. The R.M.S. error is time averaged and shown for quantum jump simulations ($\times$) and quantum state diffusion ($+$). The straight line indicates the trend of the central limit theorem, though the scaling factor is not known. In all the simulations the initial state was a 9-photon Fock state subjected to purely dissipative (1-photon) processes.

8 Entanglement in Quantum Optics

8.1 Entanglement

A composite quantum system, *i.e.* one that includes several quantum objects which are denoted subsystems, can be prepared in a so-called *entangled* state [68]. The consequences of this fact are anything but trivial and lead to various formulations of Bell's Theorem [69]. In this section we are not concerned with the widely publicized philosophical implications of Bell's Theorem and concentrate, instead, on a mathematical formulation known as the Schmidt decomposition, which apart from being a convenient mathematical tool also provides additional insights into the nature of quantum entanglement [70]. We follow in this section the presentation of Ekert and Knight [71].

Imagine two subsystems $\mathcal{U}$ and $\mathcal{V}$, with which the state spaces $\mathcal{H}_u$ and $\mathcal{H}_v$ are associated. As usual we associate the tensor product space $\mathcal{H}_u \otimes \mathcal{H}_v$ with the composite system $\mathcal{U} + \mathcal{V}$. Some state vectors of the composite system can be decomposed into a tensor product of two vectors, one describing the state of the subsystem $\mathcal{U}$ and the other describing the state of the subsystem $\mathcal{V}$, e.g.

$$|\Psi\rangle = |u\rangle \otimes |v\rangle. \tag{226}$$

However, if the two subsystems were *not* prepared independently and in total isolation from each other, in general such decomposition is impossible. For example consider a state $|\Psi\rangle$ of the composite system such that

$$|\Psi\rangle = c_1|u_1\rangle \otimes |v_1\rangle + c_2|u_2\rangle \otimes |v_2\rangle, \tag{227}$$

where

$$|c_1|^2 + |c_2|^2 = 1, \tag{228}$$

$$c_1, c_2 \neq 0. \tag{229}$$

Clearly in this case no state vector can be assigned to the subsystem $\mathcal{U}$ or $\mathcal{V}$. We call two such subsystems *entangled*. The most famous example of an entangled state of two particles is the Einstein- Podolsky- Rosen- Bohm state [72, 73] of two spin $\frac{1}{2}$ particles in the state with the total spin angular momentum zero,

$$|\Psi\rangle = \frac{1}{\sqrt{2}}(|\uparrow\rangle \otimes |\downarrow\rangle - |\downarrow\rangle \otimes |\uparrow\rangle). \tag{230}$$

The kets $|\uparrow\rangle$ and $|\downarrow\rangle$ represent states of spin-up and -down, respectively, along the arbitrary direction (e.g. along the vertical axis "z"). This state cannot be written as a simple tensor product of two states pertaining to the two particles separately.

The quantum state of one subsystem of an entangled pair (irrespective of the state of its partner) has to be described by a density operator which is a

very convenient tool that makes it possible to deal with such situations swiftly and efficiently. The density operator is a linear operator $\hat{\rho}$ in $\mathcal{H}$ such that

- $\hat{\rho}$ is Hermitian
- $\hat{\rho}$ is positive definite, that is $\langle\phi|\hat{\rho}|\phi\rangle \geq 0$ for any $|\phi\rangle \in \mathcal{H}$
- $\mathrm{Tr}\hat{\rho} = 1$

For the particular case of a state described by a state vector $|\Psi\rangle \in \mathcal{H}$, the density operator is a projection operator on that state

$$\hat{\rho} = |\Psi\rangle\langle\Psi|, \tag{231}$$

and like any projection operator is Hermitian and idempotent

$$\hat{\rho}^2 = \hat{\rho}. \tag{232}$$

A density operator can be associated with any subsystem, regardless of the existence of a state vector associated with that subsystem.

Let $\{|a_i\rangle\ i = 1, 2, 3...\}$ and $\{|b_j\rangle\ j = 1, 2, 3...\}$ form an orthonormal basis for subsystems $\mathcal{U}$ and $\mathcal{V}$ respectively. Any state $|\Psi\rangle \in \mathcal{H}$, which is a state of a composite system, can be written as

$$|\Psi\rangle = \sum_{i,j=1} c_{i,j}|a_i\rangle \otimes |b_j\rangle. \tag{233}$$

The density operator for the composite system can be put into a matrix form in this basis:

$$\begin{aligned} \hat{\rho} = \quad |\Psi\rangle\langle\Psi| \quad &= \sum_{i,j,k,l} c_{i,j}c^*_{k,l}|a_i\rangle\langle a_k| \otimes |b_j\rangle\langle b_l| \\ &= \sum_{i,j,k,l} \rho_{ij,kl}|a_i\rangle\langle a_k| \otimes |b_j\rangle\langle b_l|. \end{aligned} \tag{234}$$

Suppose that only one of the subsystems is observed and we wish to describe the properties of this subsystem regardless of the state of the other unobserved subsystems. We can assign density operators $\hat{\rho}_u$ and $\hat{\rho}_v$ to the subsystems $\mathcal{U}$ and $\mathcal{V}$ by taking a partial trace of the density operator $\hat{\rho}$,

$$\hat{\rho}_u = \quad Tr_v\hat{\rho} = \textstyle\sum_j \langle b_j|\hat{\rho}|b_j\rangle = \quad \displaystyle\sum_{i,j,k} \rho_{ij,kj}|a_i\rangle\langle a_k|, \tag{235}$$

$$\hat{\rho}_v = \quad Tr_u\hat{\rho} = \textstyle\sum_i \langle a_i|\hat{\rho}|a_i\rangle = \quad \displaystyle\sum_{i,j,l} \rho_{ij,il}|b_j\rangle\langle b_l|. \tag{236}$$

It is clear from the definition above that the partial trace operation can be applied to any density operator $\hat{\rho}$ of the composite system, not necessarily, as in our particular case, to the projection operator given by Eq.(231). For any state of the total system described by $\hat{\rho}$ and for any subsystem such as $\mathcal{U}$ or $\mathcal{V}$, we can uniquely assign the density operator that describes the state of that subsystem by taking the partial trace of $\hat{\rho}$ over all other subsystems that form the total system. This permits us to calculate all the physical predictions about the subsystems under consideration. The average value of any observable $\hat{U}$ pertaining to the subsystems $\mathcal{U}$ being in the state specified by $\hat{\rho}_u$ is given by

$$\langle \hat{U} \rangle = \mathrm{Tr}(\hat{\rho}_u \hat{U}) \tag{237}$$

8.2 The Schmidt Decomposition

We have mentioned above that any state $|\Psi\rangle \in \mathcal{H} = \mathcal{H}_u \otimes \mathcal{H}_v$, which is a state of the composite system, can be written as

$$|\Psi\rangle = \sum_{i,j=1} c_{i,j} |a_i\rangle \otimes |b_j\rangle, \tag{238}$$

or alternatively, using the density operator, as

$$\begin{aligned} \hat{\rho} = \quad |\Psi\rangle\langle\Psi| \quad &= \sum_{i,j,k,l} c_{i,j} c^*_{k,l} |a_i\rangle\langle a_k| \otimes |b_j\rangle\langle b_l| \\ &= \sum_{i,j,k,l} \rho_{ij,kl} |a_i\rangle\langle a_k| \otimes |b_j\rangle\langle b_l|. \end{aligned} \tag{239}$$

We will show now that each $|\Psi\rangle$ can be represented by a sum of bi-orthogonal terms called the Schmidt decomposition [70]. More precisely:

If the composite system is in a pure state described by a projection operator $\hat{\rho} = |\Psi\rangle\langle\Psi|$ then there exists an orthonormal basis $\{|u_i\rangle\}$ in $\mathcal{H}_u$ and $\{|v_j\rangle\}$ in $\mathcal{H}_v$, such that

$$|\Psi\rangle = \sum_i g_i |u_i\rangle \otimes |v_i\rangle, \tag{240}$$

or in terms of the density operator $\hat{\rho}$ for the entire system,

$$\hat{\rho} = \sum_{i,k} g_i g^*_k |u_i\rangle\langle u_k| \otimes |v_i\rangle\langle v_k| \tag{241}$$

where $\sum_i |g_i|^2 = 1$.

Proof

Let us choose $\{|u_i\rangle\}$ such that $\hat{\rho}_u$ is diagonal in this basis and the dimension of $\mathcal{H}_u$ is not greater than the dimension of $\mathcal{H}_v$. Let $\{|v'_j\rangle\}$ be an arbitrary basis in $\mathcal{H}_v$, then $\hat{\rho}$ can be written as

$$\hat{\rho} = |\Psi\rangle\langle\Psi| = \sum_{i,j,k,l} c_{i,j} c^*_{k,l} |u_i\rangle\langle u_k| \otimes |v'_j\rangle\langle v'_l|. \tag{242}$$

However, $\hat{\rho}_u = \sum_{ikj} c_{ij} c^*_{kj} |u_i\rangle\langle u_k|$ must be diagonal, therefore $\sum_j c_{ij} c^*_{kj} = |g_i|^2 \delta_{i,k}$. This condition allows us to switch to another orthonormal basis in $\mathcal{H}_v$. For each $|g_i| \neq 0$ and for each $|u_i\rangle$ we can define the relative state

$$|v_i\rangle = \sum_j \left(\frac{c_{ij}}{|g_i|} \right) |v'_j\rangle, \tag{243}$$

where $i = 1, 2, 3...N$, and N is not greater than the dimension of $\mathcal{H}_u$. The density operator of the composite system $\hat{\rho}$ may now be written in the following way:

$$\begin{aligned} \hat{\rho} = & \quad \textstyle\sum_{ijkl} |g_i||g_k||u_i\rangle\langle u_k| \otimes (\frac{c_{ij}}{|g_i|})|v'_j\rangle\langle v'_l|(\frac{c^*_{kl}}{|g_k|}) \\ = & \quad \textstyle\sum_{ik} |g_i||g_k||u_i\rangle\langle u_k| \otimes |v_i\rangle\langle v_k|, \end{aligned} \tag{244}$$

where only N basis vectors $\{|v_j\rangle\}$ from $\mathcal{H}_v$ are sufficient to express the state vector or the density operator of the composite system, and this completes the proof.□

A few remarks should be added here:

- The Schmidt decomposition pertains to a specific state of the composite system. For each pure state there exists the decomposition, however, for two different states $|\Psi\rangle$ and $|\Psi'\rangle$ we have two different Schmidt decompositions.

- The summation over the single index in the Schmidt decomposition goes to the smaller of the dimensionalities of the two Hilbert spaces $\mathcal{H}_u$ and $\mathcal{H}_v$. For example, when a two-state subsystem is entangled with an n-state system ($n > 2$) the Schmidt decomposition has only two terms.

- The Schmidt decomposition of a given quantum state is not unique. Our construction of the decomposition employed only the absolute values of g_i leaving the phases arbitrary. Moreover, if several $|g_i|$ are equal the corresponding vectors $|u_i\rangle \otimes |v_i\rangle$ can be replaced by linear combinations of each other. Take, for example, the EPR-Bohm singlet state [72, 73] with its spherical symmetry, which can be written in a number of forms as follows:

$$\begin{aligned}
\frac{1}{\sqrt{2}}(|\uparrow\rangle\otimes|\downarrow\rangle-|\downarrow\rangle\otimes|\uparrow\rangle) &= \\
\frac{1}{\sqrt{2}}(|\leftarrow\rangle\otimes|\rightarrow\rangle-|\rightarrow\rangle\otimes|\leftarrow\rangle) &= \\
\frac{1}{\sqrt{2}}(|\nwarrow\rangle\otimes|\searrow\rangle-|\searrow\rangle\otimes|\nwarrow\rangle) &= \\
\frac{1}{\sqrt{2}}(|\nearrow\rangle\otimes|\swarrow\rangle-|\swarrow\rangle\otimes|\nearrow\rangle). & \qquad (245)
\end{aligned}$$

The arrows illustrate different possible orientations of the spin vector showing clearly that the Schmidt decomposition is not unique. This fact causes problems in quantum measurement theory [74].

- The Schmidt decomposition *cannot*, in general, be extended to more than two subsystems.
- In the bases chosen for the Schmidt decomposition both $\hat{\rho}_u$ and $\hat{\rho}_v$ are diagonal and have the same positive spectrum. Thus any function of the density operator that depends only on the spectrum of the operator, for example the von Neumann entropy, will have the same value for $\hat{\rho}_u$ and $\hat{\rho}_v$.
- Vectors $\{|u_i\rangle\}$ and $\{|v_i\rangle\}$ define two observables $\hat{U}=\sum_i \mu_i|u_i\rangle\langle u_i|$ and $\hat{V}=\sum_i \nu_i|v_i\rangle\langle v_i|$ (eigenvalues μ_i and ν_i are arbitrary) which are perfectly correlated in state $|\Psi\rangle$. Whenever $\hat{U}$ is measured on $\mathcal{U}$ and result μ_k is obtained, then the subsequent measurement of $\hat{V}$ on $\mathcal{V}$ will, with certainty, give value ν_k. We call $\hat{U}$ and $\hat{V}$ the Schmidt observables.

Using the Schmidt decomposition we can also derive less obvious results. For example, we can easily show that any density operator pertaining to a given subsystem, here $\mathcal{U}$, can be extended to a projection operator in the state space of the composite system. It is important to realize that this is by no means the reverse of the partial trace operation. Once the partial trace of the density operator $\hat{\rho}$ has been taken and $\hat{\rho}_u$ has been obtained, there is no unique way to extend $\hat{\rho}_u$ to $\hat{\rho}$. For example, we may construct the following simple extension

$$\hat{\rho}_u \longrightarrow \hat{\rho}_u\otimes\hat{\rho}_v\,, \qquad (246)$$

where $\hat{\rho}_v$ can be any density operator in $\mathcal{H}_v$. However, much more interesting is the extension to the projection operator on the composite state space $\mathcal{H}$. We prove the following result:

For any $\hat{\rho}_u\in\mathcal{H}_u$ *there exist* $\mathcal{H}_u\otimes\mathcal{H}_v\ni\hat{\rho}=|\Psi\rangle\langle\Psi|$ *such that* $Tr_v\hat{\rho}=\hat{\rho}_u$.

Proof

Again, let $\{|u_i\rangle\}$ be a basis in which $\hat{\rho}_u$ is diagonal.

$$\hat{\rho}_u = \sum_m |g_m|^2 |u_m\rangle\langle u_m|. \tag{247}$$

According to the Schmidt decomposition theorem,

$$\hat{\rho} = \sum_{ik} g_i g_k^* |u_i\rangle\langle u_k| \otimes |v_i\rangle\langle v_k| \tag{248}$$

is a projection operator in $\mathcal{H}$, which satisfies our condition $Tr_v\hat{\rho} = \hat{\rho}_u$ and completes the proof. □

Before we analyze specific examples illustrating the usefulness of the Schmidt decomposition let us mention that subsystems which are in pure quantum states cannot be at the same time entangled with any other subsystems. For a change we will not need the Schmidt decomposition to prove this result:

If $\hat{\rho}_u$ is a projection operator which describes a pure state of $\mathcal{U}$, then the density operator of the composite system is of the form

$$\hat{\rho} = \hat{\rho}_u \otimes \hat{\rho}_v \tag{249}$$

Proof

Let us assume that the density operator assigned to $\mathcal{U}$ is a projection operator of the form

$$\hat{\rho}_u = |u_p\rangle\langle u_p|, \tag{250}$$

and let us write the density operator for the composite system using the orthonormal basis $\{|u_i\rangle \otimes |v_j\rangle \; i = 1, 2, 3..., \; j = 1, 2, 3...\}$,

$$\hat{\rho} = \sum_{ij,kl} \rho_{ij,kl} |u_i\rangle\langle u_k| \otimes |v_j\rangle\langle v_l|. \tag{251}$$

Because $\hat{\rho}_u = Tr_v\hat{\rho}$, the matrix element $\rho_{ij,kl}$ must be of the form

$$\rho_{ij,kl} = C_{jl}\delta_{ik}\delta_{ip}, \tag{252}$$

where subscript p is fixed and refers to Eq. (250).

Substituting Eq. (252) into Eq. (251) and performing the summation we obtain

$$\hat{\rho} = |u_p\rangle\langle u_p| \otimes \sum_{j,l=1} C_{jl} |v_j\rangle\langle v_l| = \hat{\rho}_u \otimes \hat{\rho}_v, \tag{253}$$

which finishes the proof. □

Last but not least, let us mention that for any entangled state of two subsystems, it is possible to find pairs of observables whose correlations violate Bell's inequality [75]. The two classes of parametrized observables are obtained as a simple modification of the perfectly correlated Schmidt observables $\hat{U}$ and $\hat{V}$.

8.3 Two-mode Squeezed State

So far we have illustrated the application of the Schmidt decomposition only with the EPR-Bohm state of two particles. Obviously this example is the most simple one. Slightly more interesting and more complicated is the case of an optical entanglement of two field modes. In a slightly over-simplified view our next example describes two quantized harmonic oscillators in a highly entangled state called the two-mode squeezed state [76] . Quite apart from its application in low-noise measurement, squeezed light is of intrinsic interest as a rare example of a realizable optical field of purely quantum character.

There are several interesting states of the single field mode such as coherent states $|\alpha\rangle$ or squeezed states $|r,\theta\rangle$,

$$|\alpha\rangle = \exp(-\frac{1}{2}|\alpha|^2)\sum_n \frac{\alpha^n}{\sqrt{n!}} \quad |n\rangle, \tag{254}$$

$$|\eta\rangle = \frac{1}{\sqrt{\cosh(r)}}\sum_n [(e^{i\theta}/2)\tanh(r)]^n \frac{\sqrt{(2n)!}}{n!} \quad |2n\rangle, \tag{255}$$

where $\eta = re^{i\theta}$.

A thermal state of a single mode with a fixed average number of photons in the mode $\langle n\rangle$, is described by a Bose-Einstein density operator which is diagonal in the Fock basis[7],

$$\hat{\rho} = \frac{1}{1+\langle n\rangle}\sum_n \left(\frac{\langle n\rangle}{1+\langle n\rangle}\right)^n \quad |n\rangle\langle n|. \tag{256}$$

The state we are going to analyze is a compound state of two subsystems (two field modes) called the two-mode squeezed vacuum state, which is the simplest version of the multimode squeezed vacuum field generated, for example, in an optical parametric amplifier. The main feature of parametric generation may be illustrated by the following example: light from a laser of frequency 2Ω is focused as the pump input into a crystal such as KDP with a large second order nonlinearity; each nonlinear interaction involves the crystal absorbing one photon from the pump laser mode and the subsequent emission of two photons into the signal and idler modes of the parametric amplifier, of frequencies ω_u and ω_v such that $\omega_u + \omega_v = 2\Omega$. The effective Hamiltonian for this interaction, involving the annihilation of a pump photon and the creation of a pair of photons in signal and idler modes, may be written as

$$\hat{H} = i\hbar\lambda(\hat{c}^\dagger \hat{a}_u \hat{a}_v - \hat{c}\hat{a}_u^\dagger \hat{a}_v^\dagger). \tag{257}$$

Here the pump field creation and annihilation operators are denoted by $\hat{c}^\dagger$ and $\hat{c}$ and λ is a measure of the strength of the nonlinear interaction (essentially governed by the size of the second order susceptibility). The intensity of the laser field is usually high. If we assume that the pumping laser produces light in a coherent state, then, to a good approximation, we may neglect the quantum character of the pumping mode and substitute the average values of $\hat{c}^\dagger$ and $\hat{c}$ instead of the operators themselves. For a coherent state this will be the amplitude of the pump E. We can then write the Hamiltonian in the much simplified quadratic form,

$$\hat{H} = i\hbar\lambda(E^* \hat{a}_u \hat{a}_v - E\hat{a}_u^\dagger \hat{a}_v^\dagger). \tag{258}$$

The evolution operator related to this Hamiltonian is

$$U(t - t_0) = \exp[\eta^* \hat{a}_u \hat{a}_v - \eta \hat{a}_u^\dagger \hat{a}_v^\dagger], \tag{259}$$

where $\eta = \lambda E(t - t_0)$, which explicitly shows that the parametric coupling in Eq.(258) is the generator of two-mode squeezing.

If at time t_0 both signal and idler modes are uncorrelated in their vacuum states, then we obtain as an output state at time t the transformed state

$$|\Psi(t_0)\rangle = |0\rangle_u \otimes |0\rangle_v \longrightarrow |\Psi(t)\rangle = \sum_n c_n |n\rangle_u \otimes |n\rangle_v, \tag{260}$$

where

$$c_n = (\cosh(r))^{-1} (\tanh(r))^n e^{in\theta} \quad ; \eta = re^{i\theta}. \tag{261}$$

In order to obtain these explicit values of coefficients c_n we can use a different parameterization of the unitary squeeze transformation. The squeeze operator that often defines two-mode squeezing or more precisely the two-mode squeezed vacuum, namely

$$|\Psi\rangle = \exp(\eta \hat{a}_u \hat{a}_v - \eta^* \hat{a}_u^\dagger \hat{a}_v^\dagger)\ |0_u\rangle \otimes |0_v\rangle. \tag{262}$$

can be, following Perelomov [77], written as

$$\begin{aligned} \exp(\eta \hat{a}_u \hat{a}_v - \eta^* \hat{a}_u^\dagger \hat{a}_v^\dagger) \quad &= \quad \left(\frac{1}{\cosh(r)}\right) \exp[-\hat{a}_u^\dagger \hat{a}_v^\dagger \tanh(r) e^{i\theta}] \times \\ &\times \exp[-(\hat{a}_u^\dagger \hat{a}_u + \hat{a}_v^\dagger \hat{a}_v) \ln(\cosh(r))] \times \\ &\times \exp[\hat{a}_u \hat{a}_v e^{-i\theta} \tanh(r)]. \end{aligned} \tag{263}$$

For the vacuum as the chosen initial state we then obtain the output as

$$|\Psi\rangle = \left(\frac{1}{\cosh(r)}\right) \exp[-\hat{a}_u^\dagger \hat{a}_v^\dagger \tanh(r) e^{i\theta}] \; |0\rangle_u \otimes |0\rangle_v. \tag{264}$$

Subsequent series decomposition of the exponent on the r.h.s. of (264) gives the required final state,

$$|\Psi\rangle = \frac{1}{\cosh r} \sum_n (\tanh r)^n e^{in\theta} |n\rangle_u \otimes |n\rangle_v. \tag{265}$$

We note that this state is already written in the Schmidt bi-orthogonal form and the basis for this decomposition is, for both modes, the well-known Fock basis representing photon number states. According to our previous observations the reduced density operators in the Fock basis are therefore diagonal, and have the form

$$\hat{\rho}_u = \sum_{n_u} \frac{1}{(\cosh(r))^2} \tanh^{2n}(r) |n_u\rangle\langle n_u|, \tag{266}$$

$$\hat{\rho}_v = \sum_{n_v} \frac{1}{(\cosh(r))^2} \tanh^{2n}(r) |n_v\rangle\langle n_v|. \tag{267}$$

At this point, we should note that the reduced density operators describe a *thermal* state of each subsystem [78, 76]. This follows from the substitution for the mean photon number $\langle n \rangle$ in terms of the amplitude r of the squeezing process (Eq.(261))

$$\langle n \rangle = \sinh^2(r), \tag{268}$$

and comparison with the corresponding expression for the mean photon number of a single mode of the field in thermal equilibrium given in Eq.(256). This result, although surprising at first, is not difficult to explain. For a pure state of the composite system, which here is made up of the two field modes, subsytems are in a maximally mixed state (compare for example the EPR state discussed in the previous section). The maximally mixed state of a single field mode with the fixed average energy is exactly the thermal state [79]. The average photon number in the mode is related to the temperature T through the Planck relation

$$\langle n \rangle = \frac{1}{\exp(\frac{\hbar\omega}{kT}) - 1}. \tag{269}$$

Last but not least, we should note that suitable experiments can use the two-mode squeezed states to test EPR correlations [80].

8.4 Entangled Fields and Atoms

The Jaynes-Cummings model (JCM) [81] is the simplest non-trivial model of the interaction between two dissimilar quantum systems; a single two-level atom interacting with a single quantised electromagnetic field mode. This model lies at the heart of laser physics and has been used for many years by theorists as a vehicle to explore fundamental ideas in quantum optics before applying such ideas in more complicated and realistic situations. The vast literature on the JCM is reviewed by Shore and Knight in [82]. Although this model is of obvious theoretical significance its interest is not solely confined to theoretical speculations. Recent experiments have demonstrated this fundamental interaction in the laboratory both in the optical regime and in the microwave regime where it forms the basis of the micromaser [83]. In the micromaser, which is the closest to the original conception of the JCM,3 an atomic Rydberg transition is employed with a transition dipole moment which is huge compared with normal optical transitions, and the single field mode is dramatically enhanced by an ultra-high Q superconducting microwave cavity. The high Q cavity essentially decouples the atom from the wider environment so that on experimentally relevant timescales the single field mode and atom entangle in isolation. One of the most interesting features of the model is the entanglement which develops between the atom and field during the interaction. This entanglement responsible for the interesting properties observed in the evolution of the micromaser, where information concerning the field is inferred by measurement of atomic properties [84].

The mathematical formalism of density operators can be in particular used to describe any two-state quantum system such as two-level atom (the most common model of atomic sources of electromagnetic fields in quantum optics [85]), photon polarization, and spin $\frac{1}{2}$ systems. Density operators of two-state systems have some additional interesting features. In the following we will use notation developed originally for spin $\frac{1}{2}$ systems, because of a convenient and enlightening description based on the SU(2) group.

The Pauli spin operators are defined through the commutation relations,

$$[\hat{\sigma}_i, \hat{\sigma}_j] = 2i\epsilon_{ijk}\hat{\sigma}_k . \tag{270}$$

In a basis in which both $\hat{\sigma}_3$ and $\hat{\sigma}^2 = \hat{\sigma}_1^2 + \hat{\sigma}_2^2 + \hat{\sigma}_3^2$ are diagonal the Pauli operators can be written in the usual matrix form

$$\sigma_1 = \begin{pmatrix} 0 & 1 \\ 1 & 0 \end{pmatrix} \quad , \quad \sigma_2 = \begin{pmatrix} 0 & -i \\ i & 0 \end{pmatrix} \quad , \quad \sigma_3 = \begin{pmatrix} 1 & 0 \\ 0 & -1 \end{pmatrix} . \tag{271}$$

Any Hermitian 2×2 matrix can be expressed in terms of the Pauli matrices together with the 2×2 identity matrix; in particular the density operator for any two-level system can be written as

Figure 27: Density matrix of a two-state system represented as the Bloch vector. The three components of vector $\vec{s} = \{s_1, s_2, s_3\}$ specify the density operator according to the parameterization $\rho = \frac{1}{2}(1 + \vec{s} \cdot \vec{\sigma})$. The two eigenvalues are $\frac{1}{2}(1 \pm |\vec{s}|)$ and the two eigenvectors are specified by the two vectors $\vec{u}$ and $-\vec{u}$; their corresponding representation in the Hilbert space is given via Eq.(273).

$$\hat{\rho} = \begin{pmatrix} \rho_{11} & \rho_{12} \\ \rho_{21} & \rho_{22} \end{pmatrix} = \frac{1}{2} \begin{pmatrix} 1+s_3 & s_1+is_2 \\ s_1-is_2 & 1-s_3 \end{pmatrix} = \frac{1}{2}(1+\vec{s}\cdot\vec{\sigma}). \tag{272}$$

For pure states $\hat{\rho}^2 = \hat{\rho} = |\Psi\rangle\langle\Psi|$, the Bloch vector $\vec{s}$ has unit length, $\sum_i |s_i|^2 = 1$, and points in some direction specified by the spherical coordinate angles θ and ϕ in the three-dimensional Euclidean space. The Bloch vector describes a quantum state which in the state space can be written as

$$|\Psi\rangle = \cos\left(\frac{\theta}{2}\right) e^{-i\phi/2}|\uparrow\rangle + \sin\left(\frac{\theta}{2}\right) e^{i\phi/2}|\downarrow\rangle. \tag{273}$$

In general, when $|\vec{s}| \leq 1$, the density operator of the form (272) has two eigenvalues

$$g_1 = \frac{1}{2}\left[1+\sqrt{s_1^2+s_2^2+s_3^2}\right] = \frac{1}{2}\left[1+|\vec{s}|\right], \tag{274}$$

$$g_2 = \frac{1}{2}\left[1-\sqrt{s_1^2+s_2^2+s_3^2}\right] = \frac{1}{2}\left[1-|\vec{s}|\right]. \tag{275}$$

and its eigenvectors are determined by two vectors $\vec{u}$ and $-\vec{u}$ in the Bloch sphere (see Fig.(1)). Vector $\vec{u}$ coincides with $\vec{s}$ for pure states *i.e.* when $|\vec{s}| = 1$ and its tip lies on the surface of the Bloch sphere. For mixed states, when $|\vec{s}| < 1$, vector $\vec{u}$ comprises vector $\vec{s}$ pointing into the same direction as $\vec{s}$ and maintaining the unit length so that its tip always lies on the surface of the Bloch sphere. Equation (273) can then be used to express $\vec{u}$ and $-\vec{u}$ in terms of the vectors in the state space.

For completeness we also introduce the usual lowering and raising operators σ and $\sigma^\dagger$ where

$$\sigma = (\sigma_1 - i\sigma_2), \tag{276}$$

$$\sigma^\dagger = (\sigma_1 + i\sigma_2). \tag{277}$$

8.5 Jaynes-Cummings Model

The single field mode of frequency ω in the JCM couples to a two level atom through the rotating-wave approximation Hamiltonian, which using the notation introduced above can be written as

$$\hat{H} = \hbar\omega_0\hat{\sigma}_3 + \hbar\omega\hat{a}^\dagger\hat{a} + \hbar\lambda(\hat{a}^\dagger\hat{\sigma} + \hat{a}\hat{\sigma}^\dagger). \tag{278}$$

The first term describes the unperturbed two-level system with a transition frequency ω_0, the second term the energy of the single mode field of frequency

ω (we have dropped the zero point energy) and the last term describes the atom-field coupling. The coupling constant λ (governed by the transition dipole moment) will lead to periodic Rabi oscillations as the atom is excited by absorption of a photon and vice-versa [85]. If the compound system of the atom and the field was initially in a pure state of the form

$$|\Psi(0)\rangle = (a|g\rangle + b|e\rangle) \otimes \sum_{n=0}^{\infty} c_n |n\rangle, \tag{279}$$

where $|g\rangle$ and $|e\rangle$ refer to the ground and the excited state of the atom respectively, and $|n\rangle$ denotes photon number states, then at any subsequent time t the state of the compound system is described by a state vector which can be written as

$$|\Psi(t)\rangle = \sum_{n=0}^{\infty} (a_n(t)|g\rangle \otimes |n\rangle + b_n(t)|e\rangle \otimes |n\rangle). \tag{280}$$

The coefficients $a_n(t)$ and $b_n(t)$ are

$$a_n(t) = ac_n \cos(\lambda\sqrt{n}t) - ibc_{n-1} \sin(\lambda\sqrt{n}t) \tag{281}$$

$$b_n(t) = bc_n \cos(\lambda\sqrt{n+1}t) - iac_{n+1} \sin(\lambda\sqrt{n+1}t). \tag{282}$$

However, according to the Schmidt decomposition, for each instant t we can always find bases, $\{|u_i(t)\rangle\}$ for the atom and $\{|v_j(t)\rangle\}$ for the field such that the state of the total system can be decomposed as [30, 86]

$$|\Psi(t)\rangle = g_1(t)|u_1(t)\rangle \otimes |v_1(t)\rangle + g_2(t)|u_2(t)\rangle \otimes |v_2(t)\rangle. \tag{283}$$

Using the time dependent bases $\{|u_i(t)\rangle\}$ and $\{|v_j(t)\rangle\}$ we can generate the reduced density matrices, which according to our previous considerations must be diagonal with the same diagonal elements. In our particular case we obtain

$$\hat{\rho}_u(t) = \begin{pmatrix} |g_1(t)|^2 & 0 \\ 0 & |g_2(t)|^2 \end{pmatrix} \quad , \quad \hat{\rho}_v(t) = \begin{pmatrix} |g_1(t)|^2 & 0 \\ 0 & |g_2(t)|^2 \end{pmatrix}. \tag{284}$$

In order to find the coefficients g_1 and g_2 together with the eigenvectors $|u_i\rangle$ and $|v_i\rangle$ we first calculate the reduced density operator for the two-level atom in the basis specified by $|g\rangle$ and $|e\rangle$,

$$\hat{\rho}_u = \begin{pmatrix} \sum_{n=0}^{\infty} |a_n(t)|^2 & \sum_{n=0}^{\infty} a_n(t) b_n^*(t) \\ \sum_{n=0}^{\infty} b_n(t) a_n^*(t) & \sum_{n=0}^{\infty} |b_n(t)|^2 \end{pmatrix}, \tag{285}$$

then following the parameterization of this density matrix in terms of the Bloch vector $\vec{s} = \{s_1, s_2, s_3\}$,

$$\hat{\rho}_u = \frac{1}{2}(1 + \vec{s}\cdot\vec{\sigma}) = \frac{1}{2}\begin{pmatrix} 1+s_3(t) & s_1(t)+is_2(t) \\ s_1(t)-is_2(t) & 1-s_3(t) \end{pmatrix}, \tag{286}$$

we can obtain the following expressions for the components $s_i(t)$,

$$s_1(t) = \sum_{n=0}^{\infty}\frac{1}{2}(a_n(t)b_n^*(t) + b_n(t)a_n^*(t)) \tag{287}$$

$$s_2(t) = \sum_{n=0}^{\infty}\frac{1}{2i}(a_n(t)b_n^*(t) - b_n(t)a_n^*(t)) \tag{288}$$

$$s_3(t) = \frac{1}{2}(|a_n(t)|^2 - |b_n(t)|^2). \tag{289}$$

The coefficients $g_1(t)$ and $g_2(t)$ can be written in terms of the length $|\vec{s}|$ of the Bloch vector,

$$g_1\ ,\ g_2 = \frac{1}{2}(1 \pm |\vec{s}|). \tag{290}$$

The two eigenvectors $|u_1\rangle$ and $|u_2\rangle$ can be also easily deduced from the Bloch vector $\vec{s}$ following the procedure described in the previous section.

It is amusing to see a field mode, traditionally described in an infinite Fock basis, reduced to a pseudo-spin in the "two-level" Schmidt basis. The length of this Bloch vector, which measures the degree of purity of a given quantum state, is also a very good measure of the entanglement of the atom and the field [30, 86, 87]. It follows from our observation in Section(5.1) that for $|\vec{s}| = 1$ the atom (or the field) is in a pure state and according to our previous general considerations it cannot be entangled with any other subsystem. This property after performing the Schmidt decomposition is clearly visible; for $|\vec{s}| = 1$ the coefficients g_1 and g_2 become 0 and 1 and the total state of the system is the direct tensor product of pure states of the two subsystems. In Fig. 28 we show the time evolution of the all three components of the Bloch vector and its norm for the atom initially in its ground state $|g\rangle$ and the field initially in a coherent state $|\alpha\rangle$, where we consider a field amplitude $|\alpha|$ such that $|\alpha|^2 = 30$.

In the Jaynes-Cummings model, the two-level atom and field periodically exchange excitation, and this leads to Rabi oscillations in the time-development of subsystem populations (component s_3 is the difference between the population in the ground state and the excited state). The frequency of the Rabi oscillations when the field is in a Fock state $|n\rangle$ and the atom is initially excited is $2\lambda\sqrt{n+1}$. If the field is actually prepared in a coherent state $|\alpha\rangle$, the Poisson distribution of photon numbers which characterize $|\alpha\rangle$ lead to a distribution of incommensurate Rabi frequencies so that the coherent oscillatory exchange collapses and partially revives as the constituent Fock components dephase and

Figure 28: Time evolution of the Bloch vector $\vec{s}(t)$ describing the Jaynes-Cummings model evolution for an atom initially in the ground state and the field in the coherent state $|\alpha\rangle$ with $\alpha = \sqrt{30}$. The upper figure shows the evolution of the inversion component s_3, while the lower figure shows that of the coherence s_1. Due to the choice of the initial conditions the coherence s_2 remains constant at zero. Time axis is labelled in dimensionless units λt.

partially rephase [88]. The collapse time is given by λ^{-1} and the revival time by $(2\pi/\lambda)\sqrt{\langle n \rangle}$.

The Fock-space solution to the JCM given in Eq.(280) has been known for many years and, of course, can be used to discuss the entire dynamics of the atom-field interaction, with its associated collapse and revivals of Rabi oscillations. As more was discovered about this fundamental model, clues to the essential two-state nature of the entangled systems were uncovered which eventually led to the use of the Schmidt basis. For example, early studies of the reduced subsystem entropies [30, 86] showed the atom and the field entropies were equal. A seminal moment in the understanding of these phenomena came with the study of the dynamics of the JCM field in phase-space by Eiselt and Risken [89]. They showed that the JCM field quasi-probabilities *bifurcate* into two components which counter-rotate with equal frequencies and amplitudes. When they are furthest apart, the Rabi oscillations collapse and only revive when the bifurcated components re-collide. In hindsight, these bifurcating quasi-probabilities, equal entropies of subsystems and the like are all characteristic signatures of the Schmidt decomposition in the JCM.

8.6 Perspective on Schmidt Decomposition

When two quantum system interact, they usually lose their individual identities within a highly correlated whole which characterizes the entangled state. We have explored the use of a pair of preferred bases, the Schmidt bases, to illustrate the nature of the entanglement between the subsystems. When the Schmidt decomposition is applied to describe a pure quantum state of the two entangled subsystems the relation between the state of the composite system and its two constituents becomes more transparent. The reduced density operators of each of the subsystems in the Schmidt bases become diagonal and with precisely the same spectrum. The smaller subsystem (*i.e.* the one with the Hilbert space of lower dimensionality) forces the bigger one to behave like the smaller one. For example, a field mode (a harmonic oscillator with an infinite number of energy eigenstates) entangles with a two-state atom ; upon entanglement it acquires something of the two-dimesionality of its entangled partner and can be described by two Schmidt states or the associated Bloch vector typical for any two-state system.

We should note that the Schmidt decomposition is useful whenever *two* subsystems become entangled, but this will not be the case when a third subsystem (or more) is introduced as this breaks the tight pairwise correlation of the states. This means that dissipation through coupling to reservoirs destroys the purity of the composite system and the one-to-one correspondence which makes the Schmidt basis so useful. However, even in this case, we can learn a lot about the subdynamics treating the reservoir as a subsystem.

8.7 Conditional measurements and entangled photon pairs

A non–degenerate paramp generates photon pairs which may be used to illustrate wide range of fundamental measurement issues [90]. One of these is the creation of modulations in conditioned measurement [91]. Consider the situation shown in Fig. 29. For reasonably weak pump fields, the relevant part of the detector plus field state vector is

$$|\Psi(0)\rangle = |1_s\rangle|1_i\rangle|d_g\rangle \tag{291}$$

where $|d_g\rangle$ is the un–excited detector and s and i stand for signal and idler. A study of the phase difference between signal and idler using the Pegg–Barnett phase operators [92] shows that $(\varphi_s - \varphi_i)$ is *random*: the detector D_1 (which is capable of counting signal photons *or* idler photons) sees *no* interferences as its position is varied along a line as shown. We now allow the detector to interact with the field described by $|\Psi(0)\rangle$ for a time t with a coupling

$$\mathcal{H}' \sim (\hat{a}_s e^{i\vec{k}_s\vec{r}_s} + \hat{a}_i e^{i\vec{k}_i\vec{r}_i})|d_e\rangle\langle d_g| + \text{ h.c.} \tag{292}$$

where $|d_e\rangle$ and $|d_g\rangle$ are the excited and ground states of the detector respectively, and r_i, r_s are distances travelled from the source to the detector by the signal and idler modes. The joint field–mode–detector state evolves in time under the influence of $\mathcal{H}'s$

$$|\psi(t)\rangle = a(t)|1_s\rangle|1_i\rangle|d_g\rangle + b(t)\{|0_s\rangle|1_i\rangle e^{i\vec{k}_s\vec{r}_s} + |1_s\rangle|0_i\rangle e^{i\vec{k}_i\vec{r}_i}\}|d_e\rangle. \tag{293}$$

But *if* a count is registered in the detector D_1, then the state of the field conditioned by this count is

$$|\psi(t)\rangle \longrightarrow \{|0_s\rangle|1_i\rangle e^{i\vec{k}_s\vec{r}_s} + |1_s\rangle|0_i\rangle e^{i\vec{k}_i\vec{r}_i}\}|d_e\rangle \tag{294}$$

This conditioned field is now disentangled from the detector, and moreover has a well–defined phase difference:

$$\langle\varphi_i - \varphi_s\rangle = \vec{k}_i \cdot \vec{r}_i - \vec{k}_s \cdot \vec{r}_s \tag{295}$$

and a variance

$$\langle\delta(\varphi_i - \varphi_s)^2\rangle = \frac{\pi^2}{3} - 2 \tag{296}$$

which should be compared with $\frac{\pi^2}{3}$ for a uniform random phase distribution. This phase coherence can be seen by a *second* detector: the count rate of a second detector D_2, given a count at the first detector at D_1 is modulated, as was seen experimentally by Ghosh and Mandel [93].

Figure 29: Production of "twin beams" by paramp with nonlinear susceptibility $\chi^{(2)}$ of pairs of down–converted photons in signal and idler modes, from a pump mode.

9 Conclusions

In these lectures we have presented a pedagogical approach to the construction of nonclassical light through quantum interference amongst component parts, and their "deconstruction" through the irreversible interaction with a dissipative environment. This allows us to investigate the evolution of single realizations of unstable quantum systems and to study the quantum jumps and the localization characteristic of particular measurement schemes, reflecting the conditioned nature of information gain from observation of individual realizations.

Acknowledgements

I thank S.M. Barnett, V. Bužek, A. Ekert, B.M. Garraway, L. Gilles, C.H. Keitel, U. Leonhard, R. Loudon, M.S. Kim, H. Moya-Cessa, I.C. Percival, D.T. Pegg, M.B. Plenio, W. Power, J. Steinbach and V. Vedral for discussions. I would like to thank in particular J. Steinbach and V. Vedral for help with these lecture notes. This work was supported in part by the European Community, the Royal Society and by the UK Engineering and Physical Sciences Research Council.

References

[1] See for example the papers reproduced in "Nonclassical Effects in Quantum Optics", eds. P. Meystre and D.F. Walls, American Institute of Physics, New York, 1991; L. Mandel and E. Wolf, "Optical Coherence and Quantum Optics", Cambridge University Press, Cambridge 1995.

[2] K. Vogel and W.P. Schleich, in "Fundamental Systems in Quantum Optics", eds. J. Dalibard, J.M. Raimond and J. Zinn-Justin (Elsevier, Amsterdam, 1991), p.713.

[3] W.H. Louisell, "Quantum Statistical Properties of Radiation", (Wiley, New York, 1974).

[4] W.H. Zurek, Phys. Today **44**, 36 (1991); W.H. Zurek, S. Habib and J.P. Paz, Phys. Rev. Lett. **70**, 1187 (1993) and refs therein.

[5] H.J. Carmichael, "An Open Systems Approach to Quantum Optics", Lecture Notes in Physics (Springer-Verlag, Berlin, 1993).

[6] M. Sargent III, M.O. Scully and W.E. Lamb Jr., "Laser Physics",(Addison-Wesley, Reading, 1975).

[7] R. Loudon, "Quantum Theory of Light", (Oxford University Press, Oxford, 1983).

[8] R. Loudon and P.L. Knight, J. Mod. Opt. **34**, 209 (1987).

[9] P. Grangier, G. Roger and A. Aspect, Europhys. Lett. **1**, 173 (1986).

[10] G.I. Taylor, Proc. Camb. Philos. Soc. **15**, 114 (1909); P.L. Knight and L. Allen, Opt. Comm. **7**, 44 (1973); M. Ley and R. Loudon, Optica Acta **33**, 371 (1986).

[11] E.P. Wigner, Phys. Rev. **40**, 749 (1932); see also M. Hillery, R.F. O'Connell, M.O. Scully and E.P. Wigner, Phys. Rep. **106**, 121 (1984).

[12] R.L. Hudson, Reports on Math. Phys. **6**, 249 (1974); N. Lütkenhaus and S.M Barnett, Phys. Rev. **A 51**, 3340 (1995).

[13] H.J. Kimble, in "Fundamental Systems in Quantum Optics", eds. J. Dalibard, J.M. Raimond and J. Zinn–Justin, Elsevier, Amsterdam ,1992.

[14] K.E. Cahill and R.J Glauber, Phys. Rev. **177**, 1857 (1969); ibid **177**, 1882 (1969)

[15] Y.S. Kim and M.E. Noz, "Phase Space Picture of Quantum Mechanics", (World Scientific, Singapore, 1991); Y.S. Kim and E. Wigner, Amer. J. Phys. **58**, 447 (1990).

[16] A.K. Ekert and P.L. Knight, Phys. Rev. **A 42**, 487 (1990); A.K. Ekert and P.L. Knight, Phys. Rev. **A 43**, 3934 (1991); see also C.W. Gardiner and M.J. Collett, Phys. Rev. **A 31**, 3761 (1985).

[17] S. Reynaud, A. Heidmann, E. Giacobino and C. Fabre, Progress in Optics **30**, (ed. E. Wolf, Elsevier, Amsterdam, 1992) and references therein.

[18] K. Vogel and H. Risken, Phys. Rev. **A 40**, 2847 (1989); see also H. Kühn, D.-G. Welsch and W. Vogel, J. Mod. Opt. **41**, 1607 (1994) and references therein.

[19] D.T. Smithey, M. Beck, M.G. Raymer and A. Faridani, Phys. Rev. Lett. **70**, 1244 (1993); M.G. Raymer,M. Beck and D.F. Mc Alister, Phys. Rev. Lett. **72**, 1137 (1994).

[20] G. Breitenbach et al, J. Opt. Soc. Am. **B 12**, 2304 (1995).

[21] E. Arthurs and J.L. Kelly, Bell. Syst. Tech. J. **44**, 725 (1965).

[22] U. Leonhardt and H. Paul, Prog. in Qu. Elect. **19**, 89 (1995).

[23] Y. Aharanov, D.Z. Albert and C.K. Au, Phys. Rev. Lett. **47**, 1029 (1981); R.F O'Connell and A.K. Rajagopal, Phys. Rev. Lett. **48**, 525 (1982); K. Wodkiewicz, Phys. Rev. Lett. **52**, 1064 (1984); K. Wodkiewicz, Phys. Lett. **115**, 304 (1986).

[24] K. Popper, "Quantum Theory and the Schism in Physics", (Hutchinson, London, 1982), p. 125–130.

[25] S. Stenholm, Eur. J. Phys. **1**, 244 (1980); S. Stenholm, Ann. Phys. (N.Y.) **218**, 233 (1992).

[26] H.P. Yuen and J.H. Shapiro, IEEE Trans. Inf. Theory **26**, 78 (1980).

[27] R. Loudon, in "Frontiers in Quantum Optics", eds. E.R. Pike and S. Sarkar, (Bristol, Adam Hilger Press, 1986), p.42.

[28] N.G. Walker, J. Mod. Opt. **34**, 15 (1987).

[29] N.G. Walker and J.E. Carroll, Electron. Lett. **20**, 981 (1987); N.G. Walker an J.E. Carroll, Opt. Qu. Electron. **18**, 355 (1986); N.G. Walker, J. Mod Opt. **34**, 15 (1987).

[30] S.J.D. Phoenix and P.L. Knight, Ann. Phys. (N.Y.) **186**, 381 (1988).

[31] V. Bužek, C. Keitel and P.L. Knight, Phys. Rev. **A 51**, 2575 and 2594 (1995).

[32] H. Araki and E. Lieb, Comm. Math. Phys. **18**, 160 (1970).

[33] A. Wehrl, Rev. Mod. Phys. **50**, 631 (1978).

[34] A. Orlowski, Phys. Rev. **A 48**, 727 (1993).

[35] K. Wódkiewicz, P.L. Knight, S.J. Buckle and S.M. Barnett, Phys. Rev. **A 35**, 2567 (1987).

[36] V. Bužek and P.L. Knight, Progress in Optics **34**, ed. E. Wolf, (Elsevier, Amsterdam, 1995) and references therein.

[37] J. Janszky, P. Domokas and P. Adam, Phys. Rev. **A 48**, 2213 (1993).

[38] V. Bužek and P.L. Knight, Opt. Comm. **81**, 331 (1991).

[39] B.M. Garraway, B. Sherman, H. Moya-Cessa, P.L. Knight and G. Kurizki, Phys. Rev. **A 49**, 535 (1994); B. Sherman and G. Kurizki, Phys. Rev. A **45**, 7674 (1992); K. Vogel, V. Akulin and W.P. Schleich, Phys. Rev. Lett **71**, 1816 (1993).

[40] J. Janszky and An.V. Vinogradov, Phys. Rev. Lett. **64**, 2771 (1990).

[41] D.F. Walls and G.J. Milburn, "Quantum Optics" (Springer-Verlag, Berlin, 1994).

[42] J.P. Paz, S. Habib and W.H. Zurek, Phys. Rev. **D 47**, 488 (1993); W.H. Zurek, Phys. Today **44**, 36 (1991); *ibid.* **46** , 84 (1993); W.H. Zurek, Prog. Theor. Phys. **89**, 281 (1993).

[43] E. Joos and H.D. Zeh, Z. Phys. **B 59**, 223 (1985); D.F. Walls and G.J. Milburn, Phys. Rev. **A 31**, 2403 (1985); S.J.D. Phoenix, Phys. Rev. **A 41**, 5132 (1990); G.J. Milburn, Phys. Rev. **A 36**, 5271 (1987).

[44] See, for example: N. Gisin, P.L. Knight, I.C. Percival, R.C. Thompson and D.C. Wilson, J. Mod. Opt. **40**, 1663 (1993) and references therein; M. Brune, S. Haroche, J.M. Raimond, L. Davidovich and N. Zagury, Phys. Rev. **A 45**, 5193 (1992); S. Haroche and J.M. Raimond, Advances in Atomic, Molecular and Optical Physics Supplement 2 (1994, Academic Press), 123–170; A. Schenzle and R.G. Brewer, Phys. Rev. **A34**, 3127 (1986).

[45] J. Dalibard, Y. Castin and K. Mølmer, Phys. Rev. Lett. **68**, 580 (1992); K. Mølmer, Y. Castin, and J. Dalibard, J. Opt. Soc. Am. **B 10**, 524 (1993); R. Dum, P. Zoller and H. Ritsch, Phys. Rev. **A 45**, 4879 (1992); Phys. Rev. **A 46**, 4382 (1992); C.W. Gardiner, A.S. Parkins and P. Zoller, Phys. Rev. **A 46**, 4363 (1992)

[46] J. Steinbach, B.M. Garraway and P.L. Knight, Phys. Rev. **A 51**, 3302 (1995).

[47] C.M. Caves and G.J. Milburn, Phys. Rev. **D 36**, 3543 (1987); L. Diosi, Phys. Rev. **A 40**, 1165 (1989); G.C. Ghirardi, P. Pearle and A. Rimini, *ibid.* **42**, 78 (1990); I.C. Percival, Proc. Roy. Soc. **447**, 189(1994); J.S. Bell, Physics World **3**, 33 (1990).

[48] G.C. Ghirardi, A. Rimini and T. Weber, Phys. Rev. **D 34**, 470 (1986).

[49] G.J. Milburn, Phys. Rev. **A 44**, 5401 (1991).

[50] H. Moya-Cessa, V. Bužek, M.S. Kim and P.L. Knight, Phys. Rev. **A 48**, 3900 (1993).

[51] H.G. Dehmelt, Bull. Am. Phys. Soc. **20**, 60 (1975).

[52] R.H. Dicke, Am. J. Phys. **49**, 925 (1981).

[53] R.J. Cook and H.J. Kimble, Phys. Rev. Lett. **54**, 1023 (1985).

[54] W. Nagourney, J. Sandberg and H.G. Dehmelt, Phys. Rev. Lett. **56**, 2797 (1986); Th. Sauter, W. Neuhauser, R. Blatt and P.E. Toschek, Phys. Rev. Lett. **57**, 1696 (1986); J.C. Bergquist, R.G. Hulet, W.M. Itano and D.J. Wineland, Phys. Rev. Lett. **57**, 1699 (1986).

[55] R.S. Van Dyck, Jr., P.B. Schwinberg and H.G. Dehmelt, Phys. Rev. Lett. **38**, 310 (1977).

[56] R. Blatt, P. Gill and R.C. Thompson, J. Mod. Opt. **39**, 193 (1992) and references therein.

[57] D.T. Pegg and P.L. Knight, Phys. Rev. A **37**, 4303 (1988).

[58] D. Bouwmeester, R.J.C. Spreeuw, G. Nienhuis and J.P. Woerdman, Phys. Rev. **A 49**, 4170 (1994).

[59] E.T. Jaynes, in "Coherence in Quantum Optics 4", eds. L. Mandel and E. Wolf, (Plenum, New York 1978).

[60] M.S. Kim and P.L. Knight, Phys. Rev. **A 36**, 5265 (1987); *ibid.* **40**, 215 (1989).

[61] M.S. Kim, B.M. Garraway and P.L. Knight, Opt. Comm. **117**, 560 (1995); see also G.C. Hegerfeldt and M.B. Plenio, Phys. Rev. **A 52**, 3333 (1995).

[62] W.L. Power and P.L. Knight, Phys. Rev **A** (1996); M.B. Plenio, P.L. Knight and R.C. Thompson, Opt. Comm **123**, 278 (1996); A. Beige, G.C. Hegerfeldt, Phys. Rev. **A 53**, 53 (1996).

[63] N. Gisin and I.C. Percival, J. Phys. **A 25**, 5677 (1992); *ibid.* **26**, 2233 (1993); *ibid.* **26**, 2245 (1993).

[64] N. Gisin and I.C. Percival, Phys. Lett. **A 167**, 315 (1992); for an alternative view, see H.D Zeh, Phys. Lett. **A 172**, 189 (1993).

[65] H.M. Wiseman and G.J. Milburn, Phys. Rev. **A 47**, 1652 (1993); see also refs. [5] and Y. Castin, J. Dalibard and K. Mølmer, in "Atomic Physics 13", eds. H. Walther, T.W. Hänsch and B. Neizert (A.I.P., New York, 1993).

[66] B.M. Garraway and P.L. Knight, Phys. Rev. **A 49**, 2785 (1994).

[67] V. Bužek, A. Vidiella-Barranco and P.L. Knight, Phys. Rev. **A 45**, 6570 (1992).

[68] The word *entanglement* is the direct translation of the German term *Verschränkung* used by Schrödinger in: E. Schrödinger, "Die gegenwärtige Situation in der Quantenmechanik", Naturwissenschaften, **23**, 807 (1935). English translation, "The Present Situation in Quantum Mechanics", Proc. of the American Philosophical Society, **124**, 323 (1980); reprinted in *Quantum Theory and Measurement* edited by J.A. Wheeler and W.H. Zurek, (Princeton, 1983) p.152.

[69] J.S. Bell, Physics **1**, 195 (1964); D.M. Greenberger, M. Horne, and A. Zeilinger, in *Bell's Theorem, Quantum Theory, and Conceptions of the Universe*, ed. by M. Kafatos, Kluwer, Dordrecht (1989) p.69. For an excellent pedagogical introduction see D.M. Greenberger, M. Horne, A. Shimony, and A. Zeilinger, Am. J. Phys. **58**, 1131 (1990).

[70] The original reference is E. Schmidt, "Zur Theorie der linearen und nicht linearen Integralgleichungen", Math. Annalen **63**, 433 (1907), in the context of quantum theory see H. Everett III, in *The Many-World Interpretation of Quantum Mechanics*, ed. B.S. DeWitt and N. Graham (Princeton University Press, Princeton, 1973) p. 3, and H. Everett III, Rev. Mod. Phys. **29** 454 (1957). A graduate level textbook by A. Peres, *Quantum Theory: Concepts and Methods*, (Kluwer, Dordrecht, 1993), Chapt. 5 includes a brief description of the Schmidt decomposition. Modern application of the Schmidt decomposition can be found in H. Huang and J.H. Eberly, J. Mod. Opt.**40**, 915 (1993); S.M. Barnett and S.J.D Phoenix, Phys Rev A **44**, 535 (1991); S.M. Barnett and S.J.D. Phoenix, Phys Lett A **167**, 233 (1992), and in Ref. [7].

[71] A.K. Ekert and P.L. Knight, Amer. J. Phys. 63, 415 (1995).

[72] A. Einstein, B. Podolsky, and N. Rosen, Phys.Rev. **47**, 777 (1935).

[73] D. Bohm, *Quantum Theory* (Prentice-Hall, Englewood Cliffs, 1951).

[74] W.Zurek, in *Quantum Optics, Experimental Gravitation, and Measurement Theory*, ed. P.Meystre and M.O.Scully (Plenum, New York, 1983) p.87.

[75] N. Gisin and A. Peres, Phys. Lett. **A 162**, 15 (1992).

[76] A.K. Ekert and P.L. Knight, Am. J. Phys. **57**, 692 (1989) and refs. therein.

[77] A. Perelomov, *Generalized Coherent States and Their Applications* (Springer, Berlin 1986).

[78] S.M. Barnett and P.L. Knight, J. Opt. Soc. Am. B **2**, 467 (1985).

[79] S.M. Barnett and S.J.D. Phoenix, Phys. Rev. **A 40**, 2404 (1989).

[80] Z.Y. Ou, S.F. Pereira, H.J. Kimble, and K.C. Peng, Phys. Rev. Lett. **68**, 3663 (1992).

[81] E.T. Jaynes and F.W. Cummings, Proc. IEEE, **51**, 89 (1963).

[82] B.W. Shore and P.L. Knight, J. Mod. Opt. **40**, 1195 (1993).

[83] D. Meschede, H. Walther, and G. Müller, Phys. Rev. Lett. **54**, 551 (1985); G. Rempe, H. Walther, Phys. Rev. Lett. **58**, 353 (1987).

[84] G. Rempe, F. Schmidt-Kaler, and H. Walther, Phys. Rev. Lett. **64**, 2783 (1990).

[85] L. Allen and J.H. Eberly, *Optical Resonance and Two-Level Atoms* (J. Wiley and Sons, Chichester, 1975).

[86] S.J.D. Phoenix and P.L. Knight, Phys. Rev.**A 44**, 6023 (1991).

[87] J. Gea-Banacloche, Opt. Comm. **88**, 531 (1992).

[88] J.H. Eberly, N.B. Narozhny, and J.J. Sanchez-Mondragon, Phys. Rev. Lett. **44**, 1323 (1980); N.B. Narozhny, J.J. Sanchez-Mondragon, and J.H. Eberly, Phys. Rev.**A 23**, 236 (1981).

[89] J. Eiselt and H. Risken, Opt. Comm. **72**, 351 (1989).

[90] L. Mandel, Phys.Scr. T **12**, 34 (1986).

[91] D.T. Pegg, Austr. J. Phys **46**, 77 (1983).

[92] D.T. Pegg and S.M. Barnett, Phys. Rev. **A 39**, 1665 (1989); S.M Barnett and D.T. Pegg, J. Mod. Opt. **36**, 7 (1989).

[93] R. Ghosh and L. Mandel, Phys.Rev.Lett. **59**, 1903 (1987).